

Mohamed Khider University of Biskra
Faculty of exact sciences and natural and life sciences
Material sciences department

MASTER MEMORY

Domain of Matter Sciences Section of Physics Speciality of Materials Physics

Réf.: Entrez la référence du document

Presented by:

Zineb Djahra

Investigation of the effects of Al, Ga, and Al/Ga codoping on the properties of ZnO thin films prepared by spray pyrolysis.

Jury:

Mrs Hamani Nadjette MCB University of Biskra Presidant

Mrs Bennaceur Kheira MCB University of Biskra Supervisor

Mrs Khater Aicha MAA University of Biskra Examiner

Academic Year: 2024 /2025

Acknowledgements

Praise be to Allah who guided me and steadied my steps, enabling me to complete this work.

I extend my sincere thanks and appreciation to Professor Bennaceur Kheira, professor at Mohamed Khider University of Biskra, for her wise guidance and meticulous supervision, which greatly enriched this research.

I also express my heartfelt gratitude to the members of the examination committee, Professor Hamani Nadjette and Professor Khater Aicha, for their cooperation and constructive evaluation.

I offer them my highest expressions of thanks and appreciation.

Dedication

Because nothing begins without roots...

To those who have been my roots in this life,

To those who taught me the true meaning of strength in gentleness, and giving in

silence,

To my mother the endless source of warmth and care,

And to my father my unwavering support and the source of my confidence at

every step,

To my family you are the beginning, the drive, and the purpose.

I dedicate every success I have achieved to you, for you are the foundation and

the extension of my journey.

TABLE OF CONTENTS

Acknowledgement	
Dedication	
General Introduction.	1
References	3
CHAPTER I: Bibliographic research	
Introduction	4
I.1. Transparent conductive oxide (TCO)	4
I.1.1 definition	4
I.1.2.Properties of Transparent Conducting Oxides (TCOs)	4
I.1.2.1.Optical Properties of TCOs	
I.1.2.2.Electrical properties.	5
I .2. Zinc oxide(ZnO)	5
1.2.1.Zinc Oxide Properties	6
I.2.1.1.Crystallographic Properties	
I.2.1.2 .Electrical Properties.	
I.2.1.3 .Optical Properties.	
I. 2.1.4.Electronic Properties and Band Structure	
I .2.2. ZnO Advantages and Selection Criteria	
I.23. Doping of ZnO	
I.2.5. Applications of Zinc Oxide	
References	
CHAPTER II: Thin films deposition techniques and cha	racterization methods
II.1. Thin Film Deposition Techniques	21
II.2.Spray Pyrolysis Technique.	21
II.3.Characterization methods.	24
II.3.1. Structural characterization.	24
II.3.1.1.X-ray diffraction (XRD)	
II.3.1.2.Lattice Parameters.	26
II.3.1.3.Strain (ε) Determination	27
II.3.1.4 .Stress (σ) Determination.	
II.3.1.5.Crystallite size.	28

II.3.2. Optical characterization.	28
II.3.2.1. UV-Visible Spectrophotometry	28
II.3.2.2. Transmittance	
II.3.2.3. Band Gap Determination.	30
II.3.2.4 .Urbach energy Determination.	31
II.3.2.5.Refractive index.	32
II.3.3. Electrical Characterization.	33
II.3.3.1. Four-point probe Method	33
II.3.3.2. Determination of Thin Film Thickness	34
II.3.3.3. Figure of merit.	34
References	36
CHAPTER III: Results and Discussion	
III.1 Preparation of ZnO, AZO, GZO, AGZO Thin Films	39
III.1.1 Experimental Conditions Before Deposition	39
III.1.2. Deposition of ZnO, AZO, GZO, AGZO Thin Films	40
III.1.3. Experimental Setup Used	42
III.2 Results and discussions	43
III.2.1.Crystal Structure Analysis Using X-ray Diffraction (XRD)	43
III.2.1.1. Crystallite Size	47
III.2.1.2. Film thickness.	49
III.2.2. Optical Analysis	50
III.2.2.1. Transmittance Spectra.	50
III.2.2.2. Urbach Energy and Optical Band Gap	51
III.2.3. Electrical Characteristics.	54
III2.3.1. Resistivity.	54
References	57
General Conclusion	

General Introduction

Zinc oxide (ZnO) has attracted considerable attention in multidisciplinary research owing to its biocompatibility and non-toxic characteristics. This versatile material finds extensive applications in diverse industrial sectors including rubber manufacturing, ceramic production, specialty chemicals, optical glass fabrication, and pharmaceutical formulations. In the field of electronics, ZnO shows excellent electrical and optical properties, and its large bandgap (3.37 eV) makes it ideal for optoelectronic applications like transparent electrodes, UV detectors, and laser diodes. The remarkable thermal and chemical stability of this transition metal oxide further expands its utility in light-emitting diodes, chemical sensors, photocatalytic systems, and radiation detectors, establishing its importance in both commercial and environmental technologies [1, 2].

As an n-type semiconductor, ZnO possesses unique electronic properties that have motivated extensive research [3]. Various deposition methods have been developed for ZnO thin film fabrication, including the sol-gel process [4], chemical vapor deposition [5], spray pyrolysis [6], and several vapor-phase deposition approaches [7].

Among these techniques, spray pyrolysis offers distinct advantages for industrial-scale production due to its operational simplicity, cost-effectiveness, and environmental friendliness. This solution-based method enables uniform large-area coatings while generating minimal waste, making it particularly suitable for commercial applications [3].

In this study, thin films of zinc oxide (ZnO) were prepared using the spray pyrolysis technique with the addition of aluminum and gallium as dopants. The effect of these dopants on the structural, optical, and electrical properties of the films was investigated.

This work is divided into three main chapters:

❖ Chapter I: This chapter discusses the general definitions and fundamental concepts of transparent and conductive oxides, in addition to their most important electrical and optical properties. It also includes a comprehensive study of zinc oxide, which is the main subject of this research, where its structural, electrical, optical, and electronic

General Introduction

- properties are identified. The chapter concludes with an overview of some potential applications of zinc oxide in various fields.
- ❖ Chapter II: This chapter discusses the definitions and concepts related to thin film preparation methods, as well as the characterization techniques used in the deposition process of these films.
- ❖ Chapter III: This chapter focuses on the experimental work conducted at the Laboratory of Thin Film Physics and Applications at the University of Biskra. It describes the properties of the equipment used in the deposition process, the procedure followed for selecting and cleaning the substrate, and the experimental conditions adopted. At the end of the chapter, the different results obtained are reviewed, compared with previous studies, and attempts are made to interpret these results.
- ❖ General Conclusion: The work concludes with a comprehensive review of the main results obtained during the research.

References:

- [1] Droepenu, E. K., Wee, B. S., Chin, S. F., Kok, K. Y., & Maligan, M. F. (2022). Zinc oxide nanoparticles synthesis methods and its effect on morphology: A review. *Biointerface Research in Applied Chemistry*, 12(3), 4261–4292.
- [2] Yang, L. (2012, September). Caractérisation de couches minces de ZnO élaborées par la pulvérisation cathodique en continu. Université du Littoral Côte d'Opale.
- [3] Ayouchi, R., Leinen, D., Martin, F., Gabas, M., Dalchiele, E., & Ramos-Barrado, J. R. (2003). Preparation and characterization of transparent ZnO thin films obtained by spray pyrolysis. *Thin solid films*, 426(1-2), 68-77.
- [4] Inna, J., Marija, M., Gundars, M., Al, ona, G. (2015). Synthesis and Properties of ZnO/Al Thin Films Prepared by Dip-Coating Process. Mater. Sci. Appl. Chem. 31, 33–38.
- [5] Wu, Z. Y., Cai, J. H., & Ni, G. (2008). ZnO films fabricated by chemical bath deposition from zinc nitrate and ammonium citrate tribasic solution. *Thin Solid Films*, 516(21), 7318–7322.
- [6] Rozati, S. M., & Akesteh, S. H. (2007). Characterization of ZnO:Al thin films obtained by spray pyrolysis technique. *Materials Characterization*, 58(3), 319–322.
- [7] Lokhande, B. J., Patil, P. S., & Uplane, M. D. (2002). Deposition of highly oriented ZnO films by spray pyrolysis and their structural, optical and electrical characterization. *Materials Letters*, 57(3), 573-579.

CHAPTER I: BIBLIOGRAPHIC RESEARCH

Introduction:

In this chapter, we provide a general definition of transparent conducting oxides (TCOs) and their key properties regarding conductivity and transparency. We then focus on zinc oxide (ZnO) as one of the most important and widely used TCOs in modern applications.

I.1. Transparent conducting oxides (TCO):

I.1.1.Definition:

Transparent conducting oxides (TCOs) are materials that exhibit electrical conductivity while maintaining relatively low absorption of electromagnetic radiation in the visible spectrum [1].

A high-quality TCO combines excellent electrical conductivity with minimal visible light absorption. These properties are largely influenced by the thickness of the deposited layer, as both conductivity and transparency depend on the grain size, which typically increases with film thickness. The most commonly used TCOs include oxides of indium, cadmium, tin, zinc, and gallium.

TCOs are often doped with metals; however, the dopant is only effective when it substitutes the host metal atom in the crystal lattice. This substitution affects the conduction band structure. Each dopant atom acts as a scattering center for conduction electrons, which can increase carrier mobility locally but generally results in a reduction in overall conductivity. To mitigate this effect, some TCOs are doped with fluorine, which improves carrier concentration and reduces resistivity. Additionally, oxygen content plays a key role in modifying the valence band structure, oxygen vacancies can reduce electron scattering and thereby enhance electrical conductivity [2].

I.1.2.Properties of Transparent Conducting Oxides (TCOs):

I.1.2.1.Optical Properties of TCOs:

A key feature of transparent conducting oxides is their optical window that spans the entire visible spectrum. Optical transmittance is defined as the ratio of the intensity of transmitted light to the intensity of incident light on the material. The absorption spectrum can be derived from both the transmission and reflection spectra [3].

The optical transparency of TCOs is primarily defined by their transmittance, which refers to the percentage of visible light that passes through the material. Both p-type and n-type

TCOs exhibit high optical transparency, typically above 80% for p-type and over 90% for n-type at a wavelength of 550 nm.

This high transparency is due to the wide band gap of these materials, which prevents them from absorbing visible light. Through doping or alloying, the band gap can be adjusted to fine-tune optical transparency in the near-infrared (NIR) or ultraviolet (UV) spectral regions [4].

I.1.2.2. Electrical properties:

The electrical behavior of TCOs is well described by the physics of wide optical band gap semiconductors. The electrical conductivity σ , expressed in $S \cdot cm^{-1}$ (or $\Omega^{-1} \cdot cm\Box^{1}$), is defined as the product of the charge carrier density n_{v} (in cm⁻³), the carrier mobility μ (in $cm^{2} \cdot V^{-1} \cdot s^{-1}$), and the elementary charge of the electron q, as described by the following equation (1):

$$\sigma = q. n_{9}. \mu \tag{I.1}$$

Electrical resistivity ρ , on the other hand, is defined as the inverse of conductivity and is expressed in $\Omega \cdot cm$:

$$\rho = \frac{1}{\sigma} \tag{I.2}$$

I.1.2.Zinc oxide:

Zinc oxide (ZnO) is a II–VI semiconductor with remarkable properties. It is a highly promising material for the development of novel materials in the fields of renewable energy and environmental applications [5]. ZnO exhibits a high exciton binding energy of 60 meV and possesses intrinsic n-type conductivity. Furthermore, it is environmentally non-toxic and abundantly available in nature, which makes it a cost-effective material [6].

In nature, ZnO occurs as the mineral zincite, typically found in the Earth's crust (Figure.I.1). However, for most technological uses, ZnO must be produced synthetically to meet specific application requirements [7].



Figure (I.1): Photographs of an orange zincite crystal [7.8].

I.2.1. Zinc Oxide Properties

I.2.1.1. Crystallographic Properties

Zinc oxide (ZnO), a II–VI compound semiconductor, exhibits a degree of ionicity that lies at the boundary between covalent and ionic semiconductors. The crystal structures of ZnO include wurtzite (B4), zinc blende (B3), and rocksalt (B1) phases, as illustrated in (Figure I.2). B1, B3, and B4 are structural designations used in the crystal structure classification system to describe these three crystallographic phases.

Under ambient conditions, the thermodynamically stable phase of ZnO is the wurtzite structure. The zinc blende structure can only be stabilized when ZnO is grown on cubic substrates [9].

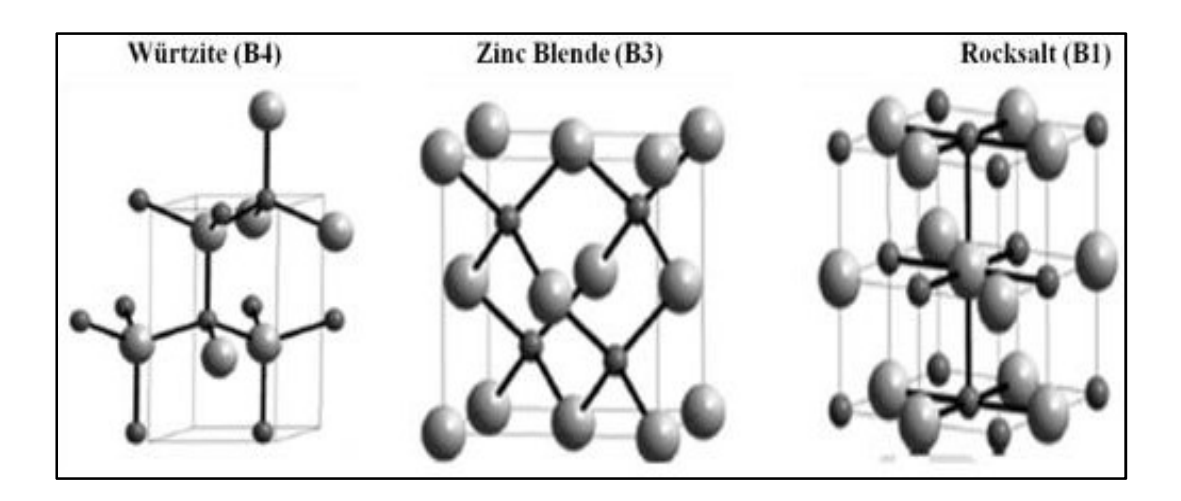


Figure (I.2): Schematic representation of the three crystallographic structures of ZnO. The small spheres represent oxygen atoms, and the large spheres represent zinc atoms [10].

The crystal structure of ZnO is characterized by the following lattice parameters:

- a = b = 3.252 Å
- c = 5.219 Å

Zinc and oxygen atoms occupy the special Wyckoff 2b positions in the P6 mc space group. Specifically, their fractional coordinates are:

- **Zn:** 0,0,0; 1/3, 2/3, 1/2
- **O:** 0,0, μ ; 1/3, 2/3, μ +1/2, with μ = 0.375

Each zinc atom is coordinated by four oxygen atoms located at the corners of a tetrahedron. However, the zinc atom is not located exactly at the center of the tetrahedron; it is displaced by 0.11 Å along the c-axis.

This structural feature allows ZnO molecules to retain a certain degree of individuality, contrary to the behavior typically expected in a purely ionic crystal. This phenomenon arises from the presence of homopolar ZnO bonds [11]. The (Figure I.3) below provides a visual representation of this distinctive structural configuration.

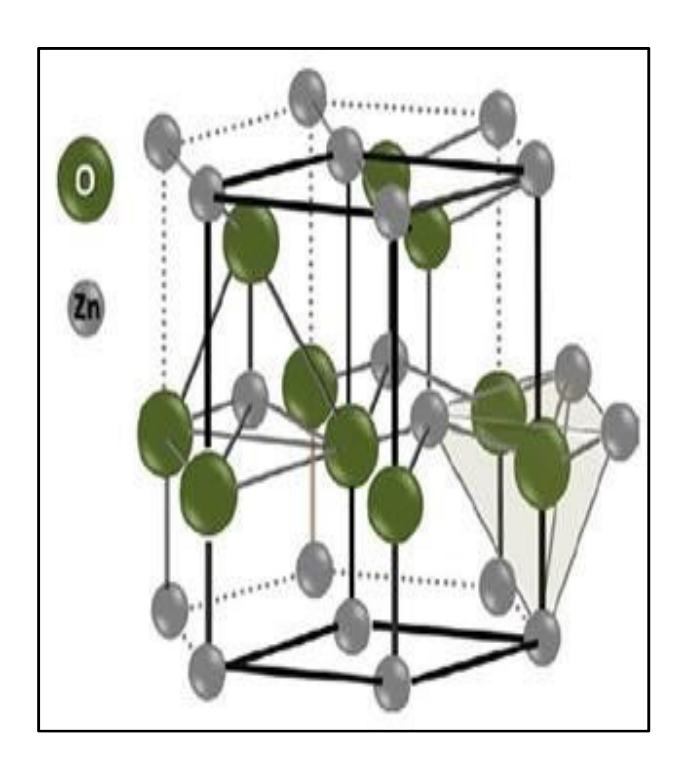


Figure (I.3): Wurtzite hexagonal crystal structure of zinc oxide[12].

I.2.1.2.Electrical Properties:

Zinc oxide (ZnO) is a semiconductor, photoconductor, and piezoelectric material, which can also function as an optical waveguide. It has a wide bandgap of approximately 3.3 eV and exhibits a high transmission coefficient of around 90% in the visible spectrum. The bandgap value can vary between 3.30 eV and 3.39 eV, depending on the preparation method and doping level [13].

The intrinsic n-type conductivity of undoped ZnO is primarily attributed to native defects such as oxygen vacancies (V_o) or zinc interstitials (Zn_i). However, for device integration and performance optimization, ZnO's electrical behavior is frequently tailored through intentional doping, which significantly modifies carrier concentration, mobility, and resistivity [14].

I.2.1.3.Optical properties:

The optical properties of materials are explained by the interaction between light, represented as an electromagnetic wave, and the electrons within the material. When applying dispersion theory to materials, it is essential to distinguish between two main types of absorption: fundamental absorption and free carrier absorption. If only fundamental absorption is present, the material is classified as a dielectric. However, if free carrier absorption is also present, the material is considered metallic or semiconducting. In semiconductors such as zinc oxide (ZnO), both fundamental and free carrier absorption play important roles. Fundamental absorption is related to electron transitions between energy bands (from the valence band to the conduction band) and accounts for absorption in the ultraviolet (UV) range, while free carrier absorption is observed in the infrared (IR) region and is linked to plasma oscillations of conduction electrons.

A semiconductor completely absorbs light when the photon energy is sufficient to transfer electrons from the valence band to the conduction band, meaning when the photon energy equals or exceeds the band gap energy.

For ZnO, the refractive index in its bulk form is approximately 2.0, but this value varies in thin films, ranging from 1.7 to 2.2 depending on the preparation methods and conditions. Improving the stoichiometry of ZnO positively affects its optical properties by reducing the absorption coefficient and increasing the band gap energy, reflecting better film quality and enhanced optical characteristics.

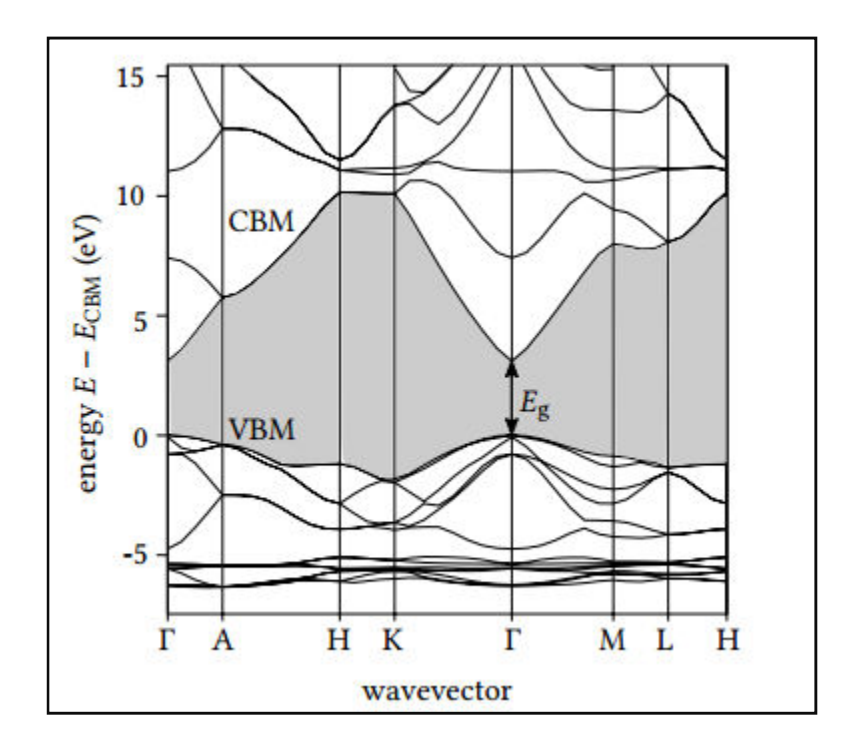
When ZnO is exposed to electromagnetic radiation with energy exceeding the band gap (greater than 3.37 eV), it emits photons through a process called photoluminescence. The emission spectra vary depending on synthesis and treatment methods, which influence the type and concentration of crystalline defects. In ZnO thin films, visible emissions mainly originate from crystal defects such as zinc interstitials and oxygen vacancies, which create deep energy levels within the band gap contributing to the luminescence [15].

I.2.1.4. Electronic Properties and Band Structure

The band structure of ZnO is presented in the first Brillouin zone. Both the maximum of the valence band and the minimum of the conduction band occur at the same point Γ (k=0), indicating that ZnO is a direct band gap semiconductor (see Figure I.5).

The bottom of the conduction band is primarily formed by the 4s level of Zn, while the top of the valence band is formed by the 2p level of O.

Experimentally, the valence band is split into three sub-bands [16].



Figure(I.4): Electronic band structure of ZnO[17].

The band gap energy (E_g) of ZnO is approximately 3.37 eV at 300 K, resulting in an absorption threshold in the near-ultraviolet region at a wavelength of around 380 nm. This band gap is the key factor in the optical and electronic properties of ZnO, as it determines the amount of energy required to excite an electron from the valence band to the conduction band [18].

I.2.2. ZnO Advantages and Selection Criteria:

Most of the recent research on ZnO materials has focused on their potential for future

applications in UV-blue light-emitting devices (LEDs) and UV-blue lasers

The most notable advantages of ZnO can be summarized as follows:

- 1. **High Exciton Binding Energy:** ZnO exhibits an exceptionally large exciton binding energy of 60 meV, significantly higher than the thermal energy at room temperature (~26 meV). This key characteristic enables the operation of UV laser diodes and other exciton-based light-emitting devices at room temperature.
- 2. **High Optical Transparency:** ZnO demonstrates excellent transparency in the visible and near-infrared spectral regions.
- 3. **High Structural Hardness:** As one of the hardest materials among II-VI compound semiconductors, ZnO possesses a high melting point and strong cohesive energy. This reduces material degradation caused by dislocation formation during device operation.
- 4. **Low Cost and Environmental Friendliness:** ZnO is cost-effective, non-toxic, and abundantly available in the Earth's crust.
- 5. **Favorable Growth Conditions:** The interfacial energy between ZnO and substrates such as sapphire or other oxides promotes two-dimensional growth, leading to high-quality films even at lower temperatures.
- 6. **High Dopability and Low Resistivity:** ZnO can be heavily doped to achieve free electron densities exceeding n > $10^{20}cm^{-3}$, resulting in low resistivity ($<10^{-3}\Omega\cdot\text{cm}$).
- 7. **Strong Electrical Contact:** ZnO provides good electrical contact with active semiconductor absorber layers.
- 8. **Large-Area Deposition Capability:** ZnO can be deposited over large areas (>1 m²) using techniques such as magnetron sputtering.
- 9. **Low-Temperature Fabrication:** ZnO films with desirable properties can be produced at relatively low substrate temperatures [1].

I.2.3. Doping of ZnO:

Doping refers to the deliberate incorporation of foreign atoms into the ZnO crystal lattice to alter its electrical, optical, or magnetic behavior. Depending on the substitution site and the type of dopant, doping in ZnO can be divided into:

a) Cationic Doping

Substitution occurs at Zn²⁺ sites using elements such as Al³⁺, Ga³⁺, In³⁺, Cd²⁺, Cu⁺, or transition metals like Fe, Co, Mn, and Ni. These dopants act as electron donors or magnetic centers, enhancing n-type conductivity or magnetic ordering.

b) Anionic Doping

Here, dopants such as N, S, F, As, or Br replace oxygen atoms. These are often used in attempts to achieve p-type conductivity, though success is limited due to compensation mechanisms.

Functional Classification:

- **a) Electronic Doping:** To enhance electrical conductivity via n-type (electron donors) or p-type (hole creators).
- b) Functional Doping: To modify optical emission, band gap energy, or magnetic response, e.g., in spintronics or UV emitters. These effects have been systematically studied for a wide range of dopant elements. For example, the incorporation of aluminum has been reported to increase the band gap of ZnO from 3.29 eV to 3.34 eV, resulting in a blue shift of both the absorption edge and the UV–Vis emission peak. Additionally, the UV-to-green emission ratio was observed to decrease following doping. Co-doping and alloying strategies have also been explored to overcome p-type doping challenges, often arising from deep acceptor levels, hydrogen contamination, and low solubility [19]. Table (I.1) summarizes doped ZnO films, showing their visible range transmittance and lowest resistivity values:

Dopant	Methods	Transmittance in visible range	Lowest resistivity	References
	Pulsed laser deposition (PLD)			[21,22]
Al	Radio-frequency(RF) magnetron sputtering	~90%	$\sim 10^{-4} \Omega \text{cm}$	[23]
	sol-gel dip-coating			[24]
Ga	PLD	~85%	$\sim 10^{-3} \Omega \text{cm}$	[25]
	chemical spray			[26]
In	chemical spray pyrolysis	~80%	~20 Ωcm	[27]
	Plasma-assisted molecular			[28]
	beam epitaxy			
N	RF magnetron sputtering	~80%	$\sim 10^{-2} \Omega \text{cm}$	[29]
	Solution processed			[30]

Table (I.1): Summary of different doped ZnO thin films as transparent conductors [20].

I.2.4.Co-Doping of Zinc Oxide (ZnO):

Several techniques have been developed to enhance the optical and electrical properties of ZnO-based transparent conducting oxides (TCOs). Among these, co-doping with solute atoms has emerged as an effective method for improving the various properties of ZnO in TCO applications. For example, ZnO thin films co-doped with aluminum and indium (Al, In) have demonstrated higher electrical conductivity compared to films doped with aluminum alone. Additionally, co-doping with vanadium has contributed to improving the thermal stability of these films.

In singly-doped ZnO, aluminum doping offers multiple advantages, including enhanced conductivity, thermal stability, and chemical stability. Meanwhile, gallium-doped ZnO (Gadoped ZnO) exhibits excellent conductivity and high resistance to humidity. Therefore, codoping with both aluminum and gallium (Al, Ga) is considered a promising approach for enhancing the overall performance of ZnO[31].

ZnO has also been co-doped with two different elements, such as magnesium and aluminum (Mg-Al), manganese and sodium (Mn-Na), and cerium and manganese (Ce-Mn)[32]. Table I.2 summarizes the electrical and optical properties of ZnO thin films co-doped with various elements.

Co-Doping Elements	Electrical Resistivity ρ (Ω·cm)	Optical Transpare ncy (T)	Band Gap Eg (eV)	References
Al/ Gd	5.28×10 ⁻⁴	88 %	3.30	[33]
Al/F	4.1 ×10 ⁻⁴	80%	3.21	[34]
Al/B	3.21 × 10 ⁻²	> 91.3%	3.28 - 3.32	[35]
Al/Ga	1.621×10 ⁻⁴ Lowest measured	80%	3.30	[36]
Al/Ti	9.1 × 10 ⁻⁴	93%	3.28	[37]

Table (I.2): Properties of ZnO Thin Films Doped with Different Elements

I.2.5. Applications of Zinc Oxide:

Zinc oxide (ZnO) is a wide-bandgap semiconductor known for its excellent transparency in both the visible and near-infrared regions of the electromagnetic spectrum. Its unique combination of properties makes it highly suitable for a wide range of technological applications.

> ZnO as a Gas Sensor

Metal oxide semiconductors such as ZnO, TiO2, and SnO2 are used in gas sensors due to their advantages, including low cost, fast response time, wide detection range, long operational life, and high sensitivity. ZnO-based sensors are fabricated in various forms, such as single crystals, pressed pellets, and thin films.

The gas sensing mechanism relies on electron trapping at adsorbed molecules and the resulting band bending, which alters conductivity. Oxygen adsorption extracts electrons, forming ions like O_2^- , O_- , and O_-^2 leading to band bending and an electron-depleted region. When the sensor is exposed to a gas containing CO, CO reacts with the adsorbed oxygen, releasing electrons and reducing the Schottky barrier, thus increasing conductivity. This mechanism applies to n-type semiconductors with depletion regions smaller than the grain size [38].

Light-Emitting Diodes (LEDs)

LEDs have been developed using both homojunctions and heterojunctions composed of different materials, exhibiting variations in performance in terms of turn-on voltage, current-voltage characteristics, and emission colors. ZnO is considered a promising candidate for blue and near-UV light sources due to its wide band gap and high exciton binding energy at room temperature, making it suitable for LED design.

Several devices based on ZnO nanostructures have been studied, where ZnO is used as an active layer in LEDs to enhance light extraction and reduce optical losses due to internal reflections. The impact of doping and different impurity incorporation methods on p-n junction formation has also been analyzed. However, homojunction LEDs based on ZnO are less common, with their performance highly dependent on the passivation layer.

Nanostructure-based LEDs offer higher efficiency compared to thin-film devices due to improved light extraction. Heterojunctions between n-type ZnO and p-type materials such as GaN have demonstrated high injection efficiency and recombination rates, enhancing overall performance.

Materials like indium tin oxide (ITO) and indium zinc oxide (IZO) are used as anodes in OLEDs, with white OLEDs proving to be highly energy-efficient, making them a viable alternative to fluorescent lighting. Additionally, aluminum-doped ZnO (AZO) is emerging as a promising indium-free transparent conducting oxide (TCO) for OLEDs applications due to its lower cost and the ability to tailor its band gap and conductivity through doping [39].

> Liquid Crystal Displays (LCDs):

Transparent conductive oxides (TCOs) are currently used in a wide range of consumer products, including liquid crystal displays (LCDs). In general, these materials are based on indium tin oxide (ITO). However, concerns regarding the limited availability of indium and its potential inability to meet future demand have driven researchers to explore cheaper and more abundant alternatives.

ZnO thin films doped with n-type donor elements such as aluminum (Al), gallium (Ga), and indium (In) have emerged as promising candidates [40].

> Solar Cells

The conversion of sunlight into electricity using photovoltaic (PV) technology has emerged as a promising solution to meet the growing global energy demands and to mitigate carbon dioxide emissions associated with fossil fuel consumption. Thin-film solar cells are particularly attractive due to their potential for low-cost, lightweight, and flexible energy generation by efficiently capturing photons from sunlight.

Zinc oxide (ZnO) has received considerable attention as a cost-effective and versatile material for photovoltaic applications. Numerous ZnO-based devices have been developed, including dye-sensitized solar cells (DSSCs) and hybrid organic—inorganic nanostructured solar cells.

ZnO contributes to photovoltaic technology in two main ways:

- As a transparent conductive oxide (TCO), ZnO is commonly used in the front electrode of solar cells, helping to reduce the shadowing effect typically caused by metallic finger contacts.
- As an n-type semiconductor, ZnO can be incorporated directly into the active layers of solar cells either as a tunnel junction in amorphous silicon solar cells or as part of the p/n junction in certain device architectures [39].

References

- [1] Bouaichi, F. (2019). Deposition and analysis of Zinc Oxide thin films elaborated using spray pyrolysis for photovoltaic applications (Doctoral dissertation, University Mohamed Khider of Biskra).
- [2] HACHOUN, Z. (2021). Performance des TCO (SnO2, In2O3, ZnO) en applications technologiques (Doctoral dissertation, Université Hassiba Benbouali de Chlef).
- [3] Tabet, A. (2013). Optimisation des conditions d'élaboration (température de substrat et distance bec-substrat) des films minces de ZnO par spray (Doctoral dissertation, Université Mohamed Khider-Biskra).
- [4] BOUNEGAB, A. (2024). Study, realization and characterization of thin films based on TCO for micro-technology applications (Doctoral dissertation, University Kasdi Merbah of Ouargla).
- [5] Habba, Y. G. (2017). Étude des nanostructures de ZnO pour leur application dans l'environnement: détection de gaz et dépollution de l'eau (Doctoral dissertation, Université Paris-Est).
- [6] Djenidi, F. (2024). L'influence de taux de dopage par Sn et Al sur les propriétés des films d'oxyde de zinc (ZnO) élaborés par spray pneumatique pour des applications photocatalytiques. (Mémoire de master, Université Mohamed Khider de Biskra).
- [7] Allag, W. (2022). *Study of thin films for photovoltaic solar cells* (Doctoral dissertation, Ferhat Abbas University Setif 1).
- [8] Ben Nouh, N., & Saidi, A. (2021). Développement de films minces d'oxydes transparents conducteurs (Doctoral dissertation, Université Kasdi Merbah Ouargla).
- [9] Morkoç, H., & Özgür, Ü. (2008). Zinc oxide: fundamentals, materials and device technology. John Wiley & Sons.
- [10] El Hallani, G. (2018). Elaboration et caractérisation de couches minces d'oxyde de zinc dopées et codopées (Al, Mg, Sn) pour des applications en photovoltaïque (Thèse de doctorat, Université Sultan Moulay Slimane).

- [11] Benramache, S. (2012). *Elaboration et caractérisation des couches minces de ZnO dopées cobalt et indium* (Doctoral dissertation, Université Mohamed Khider-Biskra).
- [12] BEN HAOUA, A. (2016). Caractérisation des couches minces de SnO2 élabore par spray ultrasonique utilisées dans les cellules solaires (Doctoral dissertation, Université Kasdi Merbah Ouargla).
- [13] BOUKHENOUFA, N. (2017). Contribution à l'étude des propriétés des films minces à base de ZnO (Doctoral dissertation, Université de Batna 2).
- [14] LEHRAKI, N. (2021). Dépôt et Caractérisation des couches minces de ZnO par spray ultrasonique (Doctoral dissertation, Université De Mohamed Kheider Biskra).
- [15] Sofiani, Z. (2007). Contributions à l'étude des propriétés optiques non linéaires de nanoparticules en couches minces à base de ZnO (Doctoral dissertation, Université d'Angers).
- [16] Guendouz, H. (2019). Elaboration et caractérisation des couches minces d'oxyde de zinc co-dopé aluminium-étain par la technique sol-gel spin coating (Doctoral dissertation, Université de JIJEL).
- [17] Deinert, J. C. (2016). Zinc oxide surfaces and interfaces: Electronic structure and dynamics of excited states (Doctoral dissertation, Technische Universität Berlin).
- [18] Taabouche, A. (2015). Etude structurale et optique de films minces ZnO élaborés par voie physique et/ou chimique (Doctoral dissertation, Université de Constantine 1).
- [19] Fang, Y. (2017). Structural parameters (size, defect and doping) of ZnO nanostructures and relations with their optical and electrical properties (Doctoral dissertation, Technische Universität Ilmenau).
- [20] OTHMANE, M. (2018). Synthesis and characterization of Zinc Oxide (ZnO) Thin films deposited by spray pyrolysis for applying: electronics and photonics (Doctoral dissertation, Universite Mohamed Khider Biskra).
- [21] Agura, H., Suzuki, A., Matsushita, T., Aoki, T., & Okuda, M. (2003). Low resistivity transparent conducting Al-doped ZnO films prepared by pulsed laser deposition. *Thin solid films*, 445(2), 263-267.

- [22] Suzuki, A., Matsushita, T., Wada, N., Sakamoto, Y., & Okuda, M. (1996). Transparent conducting Al-doped ZnO thin films prepared by pulsed laser deposition. *Japanese journal of applied physics*, 35(1A), L56.
- [23] Jeong, W. J., Kim, S. K., & Park, G. C. (2006). Preparation and characteristic of ZnO thin film with high and low resistivity for an application of solar cell. *Thin Solid Films*, *506*, 180-183.
- [24] Valle, G. G., Hammer, P., Pulcinelli, S. H., & Santilli, C. V. (2004). Transparent and conductive ZnO: Al thin films prepared by sol-gel dip-coating. *Journal of the European Ceramic Society*, 24(6), 1009-1013.
- [25] Henley, S. J., Ashfold, M. N. R., & Cherns, D. (2004). The growth of transparent conducting ZnO films by pulsed laser ablation. *Surface and coatings Technology*, 177, 271-276.
- [26] Gomez, H., Maldonado, A., Olvera, M. D. L. L., & Acosta, D. R. (2005). Gallium-doped ZnO thin films deposited by chemical spray. *Solar energy materials and solar cells*, 87(1-4), 107-116.
- [27] Kumar, P. R., Kartha, C. S., Vijayakumar, K. P., Abe, T., Kashiwaba, Y., Singh, F., & Avasthi, D. K. (2004). On the properties of indium doped ZnO thin films. *Semiconductor science and technology*, 20(2), 120.
- [28] Jiao, S. J., Zhang, Z. Z., Lu, Y. M., Shen, D. Z., Yao, B., Zhang, J. Y., Li, B. H., Zhao, D. X., Fan, X. W., & Tang, Z. K. (2006). ZnO pn junction light-emitting diodes fabricated on sapphire substrates. *Applied Physics Letters*, 88(3), 031911.
- [29] Lin, C. C., Chen, S. Y., Cheng, S. Y., & Lee, H. Y. (2004). Properties of nitrogen-implanted p-type ZnO films grown on Si 3 N 4/Si by radio-frequency magnetron sputtering. *Applied physics letters*, 84(24), 5040-5042.
- [30] Cao, Y., Miao, L., Tanemura, S., Tanemura, M., Kuno, Y., & Hayashi, Y. (2006). Low resistivity p-ZnO films fabricated by sol-gel spin coating. *Applied Physics Letters*, 88(25), 251116.

- [31] Lee, W., Shin, S., Jung, D. R., Kim, J., Nahm, C., Moon, T., & Park, B. (2012). Investigation of electronic and optical properties in Al– Ga codoped ZnO thin films. *Current Applied Physics*, 12(3), 628-631.
- [32] Aimouch, D. E., Meskine, S., Boukortt, A., & Zaoui, A. (2018). Effect of (Mn, Cr) codoping on structural, electronic and magnetic properties of zinc oxide by first-principles studies. *Journal of Magnetism and Magnetic materials*, 451, 70-78.
- [33] Anand, V., Sakthivelu, A., Kumar, K. D. A., Valanarasu, S., Ganesh, V., Shkir, M., ... & AlFaify, S. (2018). Novel rare earth Gd and Al co-doped ZnO thin films prepared by nebulizer spray method for optoelectronic applications. *Superlattices and Microstructures*, 123, 311-322.
- [34] Liu, C. F., Chen, T. H., & Huang, J. T. (2020). Effect of annealing temperature on optoelectronic performance of F- and Al-codoped ZnO thin films for photosensor applications. *Sensors and Materials*, 32(11), 3727–3736.
- [35] Tsay, C. Y., & Yu, S. H. (2021). Melioration of electrical and optical properties of Al and B co-doped ZnO transparent semiconductor thin films. *Coatings*, *11*(10), 1259.
- [36] Makuku, O., Mbaiwa, F., & Sathiaraj, T. S. (2016). Structural, optical and electrical properties of low temperature grown undoped and (Al, Ga) co-doped ZnO thin films by spray pyrolysis. *Ceramics International*, 42(13), 14581-14586.
- [37] Lin, J. C., Huang, M. C., Wang, T., Wu, J. N., Tseng, Y. T., & Peng, K. C. (2015). Structure and characterization of the sputtered ZnO, Al-doped ZnO, Ti-doped ZnO and Ti, Al-co-doped ZnO thin films. *Materials Express*, 5(2), 153-158.
- [38] Dahnoun, M. (2020). Preparation and characterization of Titanium dioxide and Zinc oxide thin films via Sol-Gel (spin coating) technique for optoelectronicapplications (Doctoral dissertation, University Mohamed Khider Biskra).
- [39] Marouf, S.(2017). *Propriétés Optiques des Nanostructures d'Oxyde de Zinc (ZnO)* (Doctoral dissertation, Université Ferhat Abbas Sétif 1).
- [40] Moezzi, A., McDonagh, A. M., & Cortie, M. B. (2012). Zinc oxide particles: Synthesis, properties and applications. *Chemical engineering journal*, *185*, 1-22.

CHAPTER II:

Deposition and Characterization Techniques of ZnO Thin Films

This chapter outlines the methodology for preparing ZnO thin films by presenting a general schematic of the main deposition techniques used in this field. Spray pyrolysis was selected as the central technique for the experimental study. The chapter also discusses the principal characterization techniques used to investigate the structural, optical, and electrical properties of the prepared films.

II.1.Thin Film Deposition Techniques:

The structural, optical, and electronic properties of thin films are largely determined by the method used during their deposition. This has led to the development of a variety of specialized techniques tailored to specific material properties and application needs. Such methods are employed to fabricate thin films composed of metals, alloys, ceramics, polymers, and superconductors on a wide range of substrates [1].

Deposition techniques are generally categorized into two main classes: physical methods and chemical methods, each offering distinct advantages in terms of control, film quality, and processing conditions.

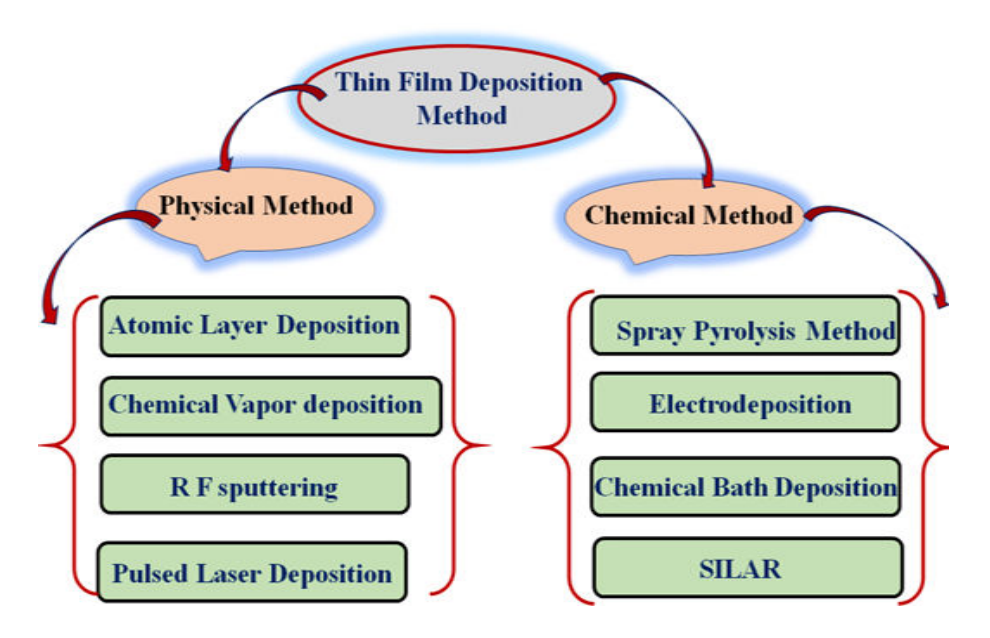


Figure (II.1): Classification of thin-film depositon techniques[2].

II.2.Spray Pyrolysis Technique

Spray pyrolysis is a straightforward, cost-effective, and scalable deposition technique widely

used for the synthesis of nanostructured metal oxides, mixed oxides, and metal-on-oxide systems [3]. It offers advantages such as reproducibility, particle size control, and the ability to operate under ambient conditions, which make it particularly attractive for large-area applications.

One of its most notable applications is in the fabrication of transparent conductive zinc oxide (ZnO) thin films. Although high-quality ZnO films with desirable electrical

and optical properties can be produced using advanced methods such as magnetron sputtering, chemical vapor deposition (CVD), or pulsed laser deposition (PLD), these approaches are expensive and require vacuum systems. Spray pyrolysis, in contrast, provides a low-cost alternative capable of delivering comparable film properties without the need for complex equipment.

The technique typically involves spraying a precursor solution, often containing zinc salts and doping agents onto a heated substrate maintained at 300–600 °C. The solution may include water, organic solvents, or a combination thereof, and additives like acetic acid are commonly introduced to stabilize the solution and prevent premature precipitation (see Figure.II.2).

A key advantage of spray pyrolysis is its ability to incorporate dopants by simply adding the desired elements to the starting solution, enabling controlled modification of the film's functional properties. The experimental setup generally includes a spray nozzle and a heated plate, allowing for uniform deposition over large areas under atmospheric pressure [4,5].

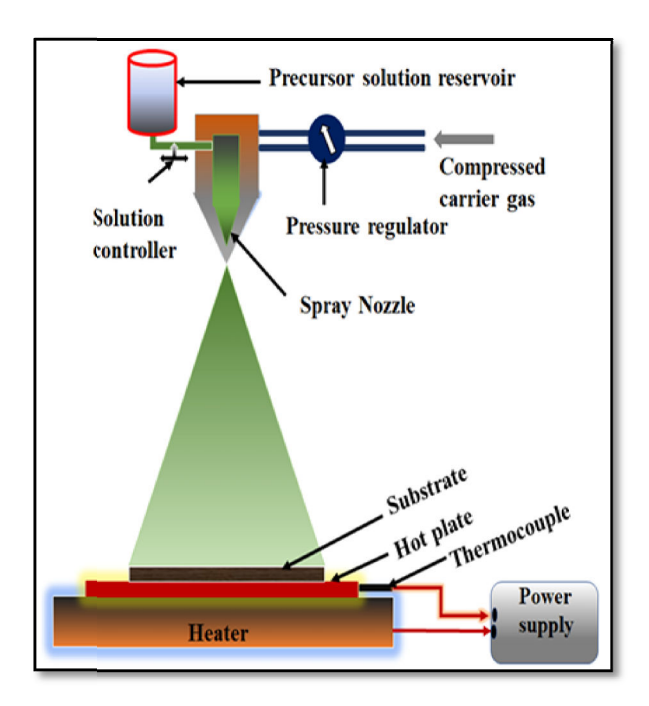


Figure (II.2): The schematics of the experimental set up for spray pyrolysis [2].

A standard spray pyrolysis system typically comprises the following components:

- **Spray device (atomizer)**: responsible for generating a fine mist of the precursor solution.
- **Precursor solution**: a homogeneous mixture containing metal salts and optional dopants dissolved in water, organic solvents, or both.
- **Heated substrate**: maintained at a controlled temperature to facilitate decomposition and film formation.
- **Temperature controller**: ensures stable and uniform thermal conditions throughout the deposition process.

Several types of atomizers are commonly employed in spray pyrolysis, each offering distinct advantages in terms of droplet size and control:

- **Air-assisted atomizer**: uses a jet of compressed air to break up the liquid stream into fine droplets.
- **Ultrasonic atomizer**: employs high-frequency ultrasonic vibrations to generate a mist of uniformly sized droplets, ideal for achieving fine and homogeneous films.

• Electrostatic atomizer (electrostatic spray technique): utilizes a high-voltage electric field to induce atomization of the liquid, offering precise control over droplet trajectory and deposition uniformity [6].

II.3.Characterization methods

Following the deposition of thin films, comprehensive characterization is essential to evaluate and optimize the key parameters influencing film quality, such as substrate temperature, dopant concentration, and precursor flow rate.

To achieve this, various analytical techniques are employed to assess the physical, structural, and chemical properties of the films [7].

II.3.1.Structural characterization

This study was conducted using X-ray diffraction with the aim of determining the structure and crystallographic growth directions of the layers, measuring the lattice parameters and the size of the crystallites. It also aims to assess the stress state within the deposited layers [7].

II.3.1.1.X-ray diffraction (XRD)

X-ray diffraction (XRD) is a widely used, non-destructive analytical method for examining the crystallographic properties of solid materials. It provides detailed information on the crystal structure, phase composition, preferred orientation (texture),

crystallite size, strain, and the presence of structural defects.

The technique is based on the interaction of incident X-ray beams with the periodic atomic planes in a crystalline material. As the X-rays are diffracted by the electrons of atoms arranged in a periodic lattice, constructive interference occurs at specific angles, as described by Bragg's law [8].

Most commonly, XRD measurements are performed using the Bragg-Brentano geometry, in which the X-ray source remains fixed while the sample rotates at an angle θ and the detector simultaneously moves at an angle 2θ . The resulting diffraction pattern shown in

Figure (II.3) is recorded as the intensity of the diffracted beam versus the 2θ angle, allowing for the identification and analysis of the material's structural characteristics [9].

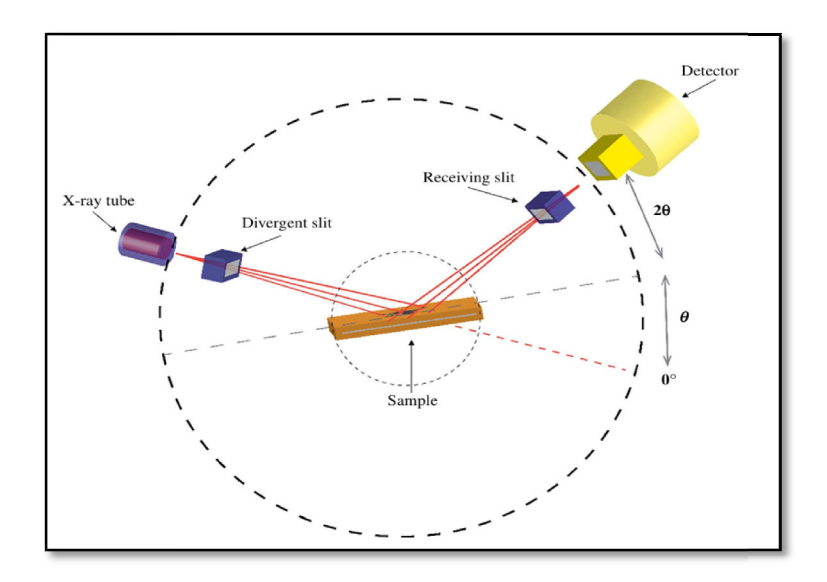


Figure (II.3): Schematic illustration of X-ray diffractometer instrument[10].

When X-rays interact with a crystalline material, they are scattered by the periodic array of atoms. Constructive interference of the scattered waves occurs only at specific angles, which satisfy **Bragg's Law** (see figure.II.4):

$$n\lambda = 2d_{\square kl} \sin \theta \tag{II.1}$$

Where:

- d_{hkl} is the spacing between crystallographic planes indexed by Miller indices (hkl),
- θ is the angle of incidence (also the diffraction angle),
- λ is the wavelength of the incident X-ray beam,
- **n** is the order of diffraction (an integer, typically n=1).

This condition defines the angles at which the intensity of the diffracted X-ray beam is enhanced due to constructive interference, and it forms the basis for determining the crystallographic structure of materials [7].

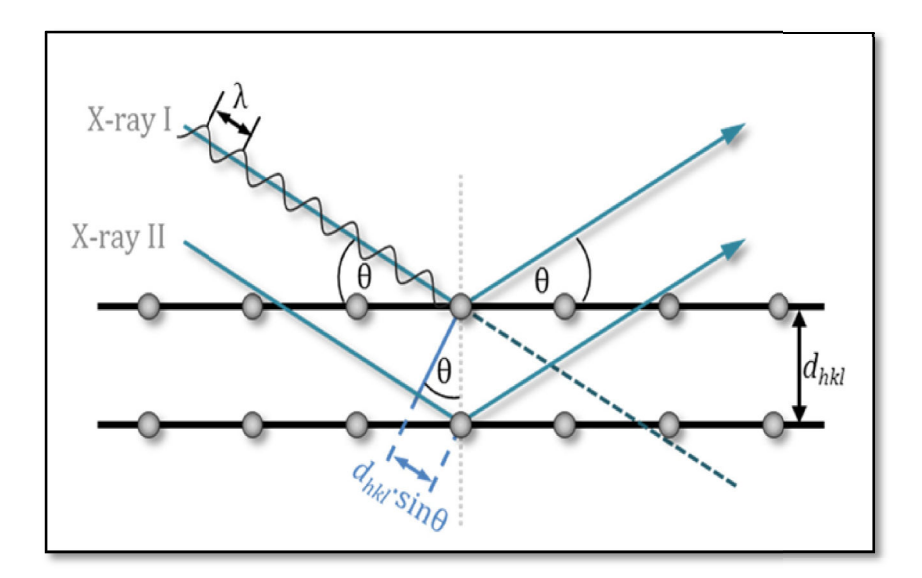


Figure (II.4): Schematic representation of Bragg equation [11].

II.3.1.2.Lattice Parameters

Lattice parameters describe the physical dimensions of a unit cell in a crystal. For hexagonal structures such as zinc oxide (ZnO), two primary parameters define the cell: a (the basal plane dimension) and c (the vertical axis). These parameters can be extracted from X-ray diffraction data by analyzing the interplanar spacing d_{hkl} using Bragg's Law in combination with the following relation specific to hexagonal systems:

$$d_{hkl} = \frac{a}{\sqrt{\frac{4}{3}(h^2 + k^2 + \Box k) + l^2 \frac{a^2}{c^2}}}$$
 (II. 2)

Where:

- d_{hkl} is the interplanar spacing corresponding to the (hkl) planes,
- a and c are the lattice constants,
- **h**, **k**,**l** are the Miller indices of the diffraction plane.

This equation allows precise calculation of the lattice parameters from experimental XRD data [12].

II.3.1.3.Strain (ε) Determination

Strain (ϵ) quantifies the relative deformation of the ZnO crystal lattice, often induced by intrinsic or extrinsic stresses during thin film deposition. For ZnO in the wurtzite structure, strain is typically assessed along the c-axis by comparing the lattice parameter of the film to that of bulk ZnO:

$$\varepsilon = \frac{c_{film} - c_0}{c_0} \times 100\% \tag{II.3}$$

Where:

- c_{film} is the out-of-plane lattice constant of the deposited film, typically derived from the (002) reflection in the XRD pattern,
- c_0 is the reference lattice parameter for bulk ZnO (≈ 0.5206 nm).
- A positive ε indicates tensile strain, whereas a negative ε signifies compressive strain along the c-axis [13].

II.3.1.4.Stress (σ) Determination

Stress (σ) in ZnO thin films is evaluated using Hooke's law adapted to hexagonal crystal systems. The mechanical stress resulting from the lattice mismatch or thermal expansion can be estimated from the strain using the film's elastic constants. Stress formula using stiffness constants:

$$\sigma = \left[2. C_{13} - \frac{(C_{11} + C_{12}).C_{33}}{2.C_{13}}\right] \times \epsilon$$
 (II. 4)

Where:

- C11=209.7 GPa
- C12=121.1 GPa
- C13=105.1 GPa
- C33=210.9 GPa

These elastic constants define the stiffness of ZnO along different crystallographic axes and are essential for accurate stress quantification [14].

II.3.1.5. Crystallite size

The crystallite size of ZnO thin films was estimated using the well-known Debye-Scherrer formula

$$G = \frac{0.9\lambda}{\beta \cos \theta}$$
 (II. 5)

Where **G** is the crystallite size, λ is the wavelength of the X-ray ($\lambda = 1.5406$ Å), β is the full width at half maximum (FWHM) of the diffraction peak in radians, and θ is the Bragg angle corresponding to the peak position [13].

Φ Determination of Dislocation Density (δ)

Dislocation density (δ) refers to the total length of dislocation lines per unit volume within a crystalline material. It serves as an indicator of the degree of crystalline imperfection.

In this study, δ was estimated using the Williamson and Smallman relation, which correlates the dislocation density with the crystallite size (G) as follows:

$$\delta = \frac{1}{G^2} \tag{II.6}$$

The resulting dislocation density is usually expressed in units of lines per square meter (m⁻²) [15].

II.3.2.Optical characterization

II.3.2.1.UV-Visible Spectrophotometry

UV-Visible spectrophotometry is a widely used analytical technique for assessing the optical behavior of materials. It enables the evaluation of fundamental properties such as light transmission, absorption spectra, and optical band gap energy. Additionally, it can be employed to estimate crystallite sizes and, under certain conditions, the film thickness of the sample [16].

***** Working principle

The operation of UV-Visible spectrophotometry is grounded in the electronic transitions that occur when molecules absorb photons, causing electrons to move from a lower (ground) energy level to a higher (excited) state.

The instrument typically uses two light sources:

- A deuterium lamp for the ultraviolet range (180–400 nm)
- A tungsten lamp for the visible range (400–800 nm)

A monochromator isolates the desired wavelength of light, which is directed via mirrors to ensure beam alignment. The beam then passes through the test sample or a reference (see Figure II.5). The instrument compares the intensity of the transmitted light with that of the incident beam to quantify absorbance or transmittance [17].

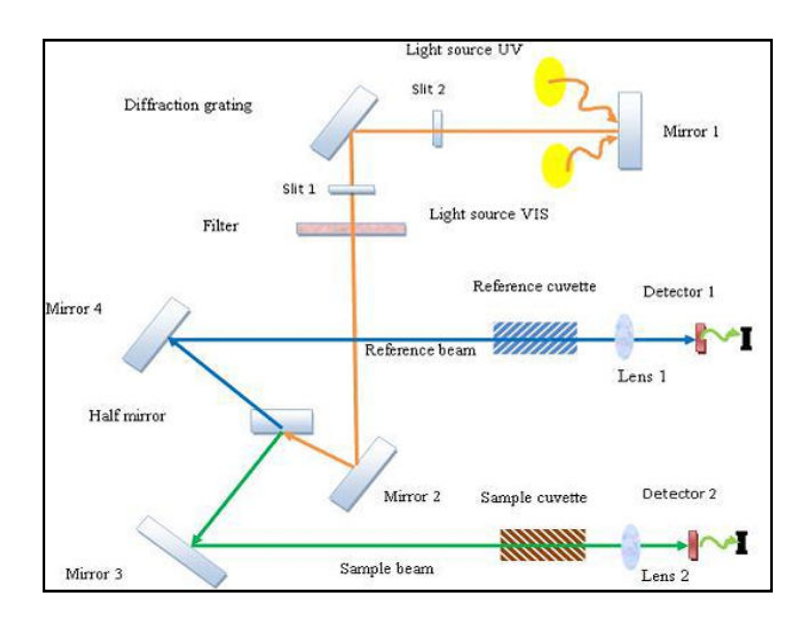


Figure (II.5): The operating principle of UV-Visible spectroscopy [18].

UV-Visible spectroscopy is based on the interaction between electromagnetic radiation and matter. When light in the ultraviolet or visible range strikes a sample, part of it is absorbed while the remainder is transmitted. The absorption of photons leads to electronic transitions within atoms, ions, or molecules, where electrons are promoted from lower to higher energy levels [16].

II.3.2.2.Transmittance

Consider a homogeneous material of thickness d, subjected to a light beam of initial intensity $I\Box$ incident perpendicular to the sample surface. The transmitted intensity I is described by the Beer–Lambert law:

$$I = I_0 e^{-\alpha d} \tag{II.7}$$

Where:

• α is the absorption coefficient (in cm⁻¹), which depends on the material and the wavelength of the incident light.

The absorption coefficient is related to the extinction coefficient (**K**) by the expression:

$$\alpha = \frac{4\pi K}{\lambda} \tag{II.8}$$

Where, λ is the wavelength of the light used [19].

Once the intensity of light after it passes through the cuvette is known, it can be related to transmittance (T). Transmittance is the fraction of light that passes through the sample. It can be calculated using the following equation [20]:

$$T = \frac{I_t}{I_0}$$
 (II. 9)

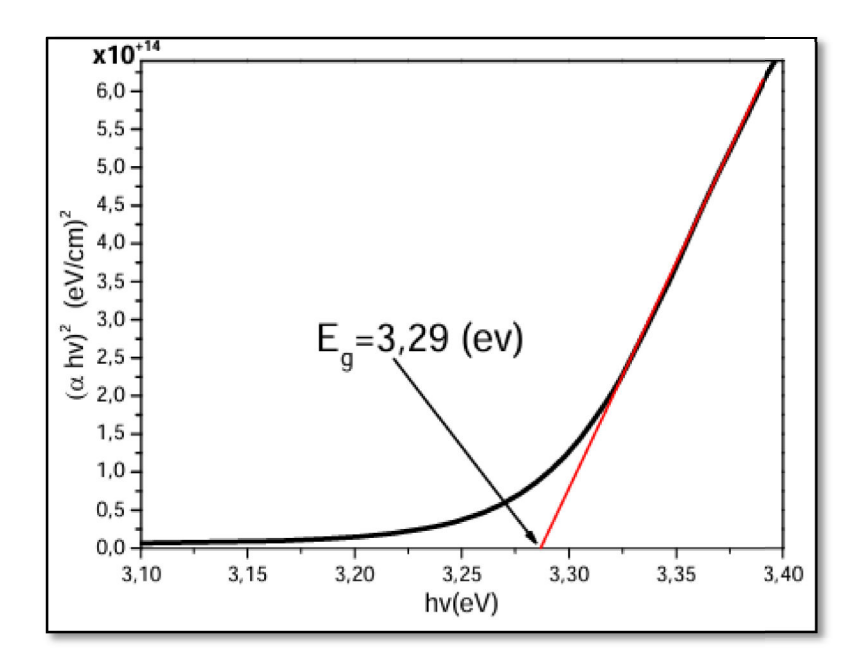
II.3.2.3.Band Gap Determination

The optical band gap energy (Eg) of a material can be estimated from its transmittance spectrum using Tauc's method:

$$(\alpha h \nu)^2 = A(h \nu - Eg)$$
 (II. 10)

Where α denotes the absorption coefficient of the material, $h\nu$ is the photon energy, A is a constant and Eg represents the optical band gap.

The band gap was estimated under the assumption of a direct allowed electronic transition between the valence and conduction bands, by extrapolating the linear region of the Tauc plot $(\alpha h\nu)^2$ versus $h\nu$ to the energy axis, at the point where $(\alpha h\nu)^2 = 0$ [21].(see Figure.II.6).



Figure(II.6): Variation of $(\alpha h \nu)^2$ as a function of $(h \nu)$ for the ZnO thin film[22].

II.3.2.4. Urbach energy Determination

In the region near the absorption edge, the absorption coefficient α exhibits an exponential dependence on photon energy (hv), a behavior described by the Urbach energy (Eu). This parameter is associated with the width of the band tails arising from localized states, which are linked to structural disorder, lattice imperfections, and other microstructural defects [23].

The Urbach relation is expressed as:

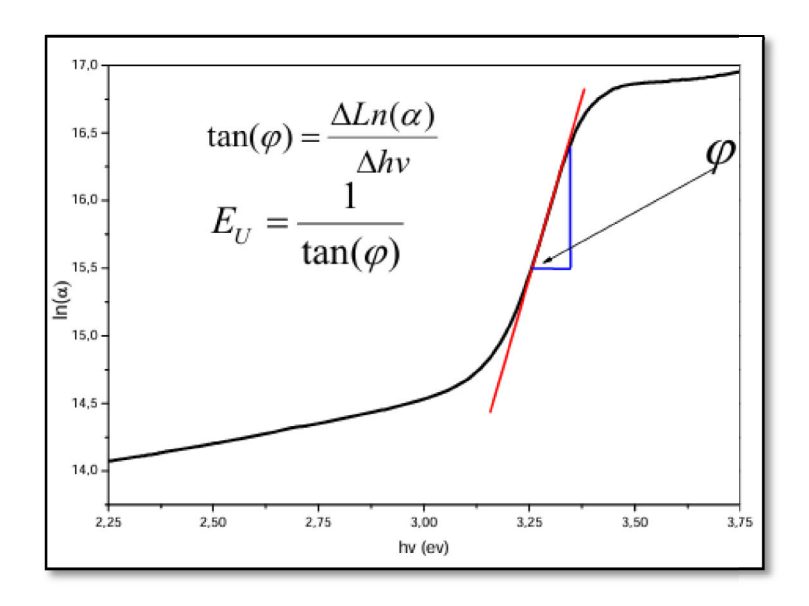
$$\alpha = \alpha_0 \exp\left(\frac{h\nu}{E_u}\right) \tag{II. 11}$$

Where α_0 is constant.

Taking the natural logarithm of both sides yields [15]:

$$ln\alpha = ln\alpha_0 + \frac{h\nu}{E_u}$$
 (II. 12)

This linear form indicates that a plot of $ln(\alpha)$ versus $h\nu$ will produce a straight line in the exponential tail region, from which the Urbach energy Eu can be extracted as the inverse of the slope Figure (II.7).



Figure(II.7): Variation of the absorption coefficient (α) as a function of photon energy (hv)[22].

Urbach energy has units of electron volts (eV) and serves as an indicator of the degree of disorder within the material. In ZnO thin films, higher values of Eu suggest increased structural imperfections, such as dislocations, point defects, and compositional fluctuations. These defects introduce localized energy levels that broaden into tails, sometimes merging with the conduction band due to donor level overlap and impurity band formation [24].

II.3.2.5.Refractive index

Extensive research has demonstrated a strong correlation between the refractive index and the optical band gap of semiconductors. This relationship serves as a basis for estimating the refractive index across various semiconductor classes. Among the most commonly applied empirical models are:

(a) Ravindra relation[25]:

$$n = 4.084 - 0.62E_g \tag{II. 13}$$

(c) Herve-Vandamme model [26]:

$$n^2 = 1 + \left(\frac{A}{E_g + B}\right)^2 \tag{II. 14}$$

Where A and B are constants with values A = 13.6 eV and B = 3.4 eV.

II.3.3. Electrical Characterization

II.3.3.1.Four-point probe Method

The electrical resistivity of the prepared thin films was measured using a LUCAS LABS-302 SYSTEM four-point probe setup. This technique employs a probe with four equally spaced tungsten tips (s = 1 mm) arranged in a straight line on the sample surface.

In this configuration, the two outer probes are used to inject a constant current (I), while the two inner probes measure the resulting voltage drop (U) across the sample. This arrangement minimizes the influence of contact resistance and allows for accurate determination of the film's resistive properties [27].

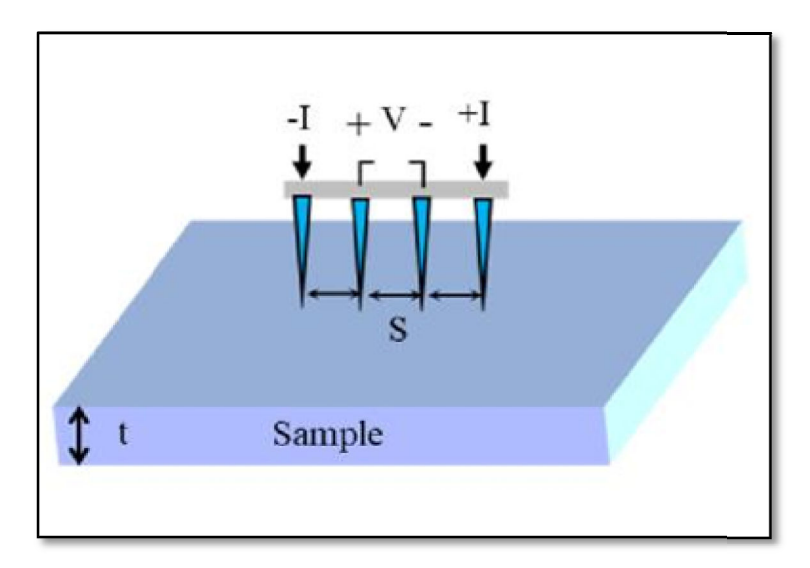


Figure (II.8): Schematic of the in-line 4point probe to measure R_{sh} [28].

When the distance s between the terminals is much greater than the thickness of the thin film ($t \ll s$), the lateral dimensions can be considered infinite, and the resistivity of the layer can be deduced using the formula(II. 15):

$$\rho = R_{sh}.t \tag{II.15}$$

Where R_{sh} is the sheet resistance, calculated by the ratio U/I multiplied by a correction factor that accounts for the finite dimensions of the sample [28]. This correction factor is given by the following formula(II. 17):

$$R_{\rm sh} = \frac{\pi}{\ln 2} \frac{U}{I} \tag{II. 16}$$

II.3.3.2.Determination of thin film thickness

In this study, The thickness of the deposited thin film can measured using the weight difference technique (Eq. II. 18), which is easy and practical [29].

$$t = \frac{\Delta m}{\rho \cdot s} \tag{II. 17}$$

Where

- ρ denotes the bulk density of the material.
- Δm is the difference in the substrate mass before (cleaned substrate) and after (substrate + thin film) the deposition.
- S is the deposited surface.

II.3.3.3.Figure of merit

The concept of the figure of merit was first introduced by Fraser and his colleagues as an index known as FOM. It was later developed by Haacke and his team to express material efficiency through the ratio of transmittance to the sheet resistance of the layer, according to the equation:

$$FOM = \frac{T^{10}}{R_{sh}}$$
 (II. 18)

Where T represents transmittance and R_{sh} represents sheet resistance. The higher the value of FOM, the greater the material efficiency.

This equation is specifically used to evaluate Transparent Conducting Oxides (TCOs), which must combine high conductivity with low light absorption in the visible range, making FOM an important criterion in optoelectronic applications [30].

References

- [1] Benkheta, Y. (2019). Elaboration and characterization of thin layers of zinc oxide (ZnO) deposited by ultrasonic spray for photovoltaic and optoelectronic applications (Doctoral dissertation, University Mohamed Khider of Biskra).
- [2] Sawant, J. P., Pathan, H. M., & Kale, R. B. (2021). Spray pyrolytic deposition of CuInS2 thin films: properties and applications. *Engineered Science*, *13*, 51-64.
- [3] Ghaffarian, H. R., Saiedi, M., Sayyadnejad, M. A., & Rashidi, A. M. (2011). Synthesis of ZnO nanoparticles by spray pyrolysis method. *Iranian Journal of Chemistry and Chemical Engineering*, 30(1), 1–6.
- [4] Zhou, B. (2013). Codoped Zinc Oxide by a Novel Co-Spray Deposition Technique for Solar Cells Applications. (Doctoral dissertation, Arizona State University).
- [5] Perednis, D. (2003). Thin film deposition by spray pyrolysis and the application in solid oxide fuel cells (Doctoral dissertation, ETH Zurich).
- [6] Bouhssira, N. (2013). Elaboration des films minces d'oxyde de zinc par évaporation et par pulvérisation magnétron et étude de leurs propriétés (Doctoral dissertation, University of Constantine 1).
- [7] Kouidri, N. (2019). Contribution à l'étude de couches minces d'oxydes transparents conducteurs à base de zinc et cobalt par spray pneumatique (Doctoral dissertation, University of Mohamed Khider, Biskra).
- [8] Lee, J. J. (2014). The development of transition metal and rare earth codoping ZnO for spintronics application (Doctoral dissertation, UNSW Sydney).
- [9] Ammar, D. (2011). L'effet de la distance du Bec et la température du substrat sur les propriétés des couche minces d'oxyde de zinc (ZnO) (Doctoral dissertation, Université Mohamed Khider de Biskra).
- [10] Falsafi, S. R., Rostamabadi, H., & Jafari, S. M. (2020). X-ray diffraction (XRD) of nanoencapsulated food ingredients. In S. M. Jafari (Ed.), *Characterization of nanoencapsulated food ingredients* (pp. 271–293). Academic Press.

- [11] Paula, C. (2021). In situ solid-state NMR and XRD investigations of structural transformations in crystalline porous solids (Doctoral dissertation, Friedrich-Alexander-Universität Erlangen-Nürnberg (FAU)).
- [12] KABOT, O., & MERIZIG, M. (2022). L'effet de la température de recuit sur les propriétés des couches minces de ZnO: Al déposées par spray pneumatique. (*Mémoire de master, Université Mohamed Khider de Biskra*).
- [13] Aoun, Y., Benhaoua, B., Gasmi, B., & Benramache, S. (2015). Study the structural, optical and electrical properties of sprayed Zinc oxide (ZnO) thin films before and after annealing temperature. *Main Group Chemistry*, 14(1), 27-33.
- [14] Moustaghfir, A. (2004). Elaboration et caractérisation de couches minces d'oxyde de zinc. Application à la photoprotection du polycarbonate (Doctoral dissertation, Université Blaise Pascal-Clermont-Ferrand II).
- [15] Bennaceur, K. (2020). *Elaboration and characterization of SnO2: In thin films deposited by spray pyrolysis technique* (Doctoral dissertation, University Mohamed Khider Biskra).
- [16] Ghomri, R. (2017). Étude des propriétés de l'oxyde de zinc non dopé et dopé. (Doctoral dissertation, Université Badji Mokhtar Annaba).
- [17] Louiza, A. (2012). Elaboration par différentes méthodes et étude optique des poudres nanocristallines de ZnO pur et dopé par différents oxydes (Thèse de Doctorat, Université de Constantine).
- [18] Amri, A. (2024). Elaboration des couches minces à base de ZnO pour transistors couches minces TFTs (Doctoral dissertation, Université Mohamed Khider Biskra).
- [19] Rahmane, S. (2008). Élaboration et caractérisation de couches minces par spray pyrolyse et pulvérisation magnétron (Doctoral dissertation, Université Mohamed Khider Biskra).
- [20] Sanda, M. F., Victor, M. E., Monica, T. A., & Alina, C. (2012). Base theory for UV-Vis spectrophotometric measurements. University of Oradea.

- [21] Gong, L., Lu, J., & Ye, Z. (2011). Conductive Ga doped ZnO/Cu/Ga doped ZnO thin films prepared by magnetron sputtering at room temperature for flexible electronics. *Thin Solid Films*, *519*(11), 3870-3874.
- [22] Boulmelh, S. (2015). Élaboration et caractérisation d'un dépôt de couches minces d'oxyde de zinc par spray pyrolyse (Mémoire de magister, Université de Frères Mentouri Constantine).
- [23] Norouzzadeh, P., Mabhouti, K., Golzan, M. M., & Naderali, R. (2020). Investigation of structural, morphological and optical characteristics of Mn substituted Al-doped ZnO NPs: A Urbach energy and Kramers-Kronig study. *Optik*, 204, 164227.
- [24] Vettumperumal, R., Kalyanaraman, S., Santoshkumar, B., & Thangavel, R. (2016). Estimation of electron–phonon coupling and Urbach energy in group-I elements doped ZnO nanoparticles and thin films by sol–gel method. *Materials Research Bulletin*, 77, 101-110.
- [25] Ravindra, N. M., Auluck, S., & Srivastava, V. K. (1979). On the Penn gap in semiconductors. *Physica status solidi (b)*, 93(2), K155-K160.
- [26] Herve, P. J. L., & Vandamme, L. K. J. (1995). Empirical temperature dependence of the refractive index of semiconductors. *Journal of Applied Physics*, 77(10), 5476-5477.
- [27] Medjnoun, K. (2015). Etude et réalisation de semi-conducteurs transparents ZnO dopé vanadium et oxyde de vanadium en couches minces pour applications photovoltaïques (Doctoral dissertation, Université Mouloud Mammeri).
- [28] Habis, C. (2022). Development of ZnO-FTO nanocomposites for the use in transparent conductive thin films (Doctoral dissertation, Université de Lorraine).
- [29] BESRA, S. (2023). Synthesis and characterization of thin films based on functional metal oxides (Doctoral dissertation, Université Kasdi Merbah Ouargla).
- [30] BEN HAOUA, A. (2016). Caractérisation des couches minces de SnO2 élabore par spray ultrasonique utilisées dans les cellules solaires (Doctoral dissertation, Université Kasdi Merbah Ouargla).

CHAPTER III: RESULTS AND DISCUSSION

This chapter provides the experimental details of depositing ZnO, ZnO:Al (AZO), ZnO:G (GZO), and ZnO:(Al,Ga) (AGZO) thin films, including the selection and preparation of substrates and precursor solutions. The apparatus used, as well as the deposition procedures, are described in detail. Finally, the structural, electrical, and optical properties of the ZnO, AZO, GZO, and AGZO thin films are examined.

III.1. Preparation of ZnO, AZO, GZO, AGZO Thin Films

III.1.1.Experimental conditions before deposition

> Substrate Selection

Glass slides measuring 25 mm \times 15 mm were selected as the substrate and were cut using a diamond-tipped cutter.

> Reasons for selecting glass as a substrate

- Glass has a thermal expansion coefficient similar to that of ZnO, which helps minimize thermal stress at the interface.
- Its high transparency makes it suitable for optical analysis in the visible light range.
- Glass is cost-effective and readily available, making it a practical and economical choice for thin-film deposition research and applications.

> Substrate Cleaning

Given the direct impact of the substrate's cleanliness and surface condition on the quality of the deposited layer, and subsequently on the overall performance of the sample, the cleaning process of the substrate is a critical step that requires careful attention. This process aims to remove any surface contaminants such as grease or dust, while also ensuring that the substrate surface is free from scratches or flatness defects through visual inspection.

This step is essential to ensure strong adhesion of the deposited layer and uniform thickness across the substrate.

Therefore, the glass substrate is selected and cleaned according to the following protocol:

- Clean the substrate using soapy water or a detergent, followed by rinsing with distilled water for 10 minutes.
- Clean the substrate with acetone
- Rinse the substrate with distilled water
- Clean the substrate with ethanol for 5 minutes at room temperature to remove any traces of grease and impurities.
- Rinse the substrate with distilled water
- Dry the substrate using an air blower, ensuring not to touch the surface to avoid contamination.

III.1.2. Deposition of ZnO, AZO, GZO, AGZO Thin Films

Undoped, doped, and co-doped zinc oxide (ZnO) thin films were deposited via spray pyrolysis technique. Aluminum (Al) and gallium (Ga) dopants were introduced separately, each at 1 wt.%, and the co-doped films contained both Al and Ga, each at 1 wt.%. Zinc acetate monohydrate (Zn(CH₃COO)₂.H₂O) was used as the precursor for ZnO, with aluminum chloride hexahydrate (AlCl₃.6H₂O) and gallium nitrate nonahydrate (Ga(NO₃)₃.9H₂O) serving as the dopants for Al and Ga, respectively, to produce AZO and GZO films. The precursor solutions were dissolved in distilled water and sprayed onto glass substrates heated to 400°C.

The films were deposited under controlled parameters, with the spray nozzle-substrate distance maintained at 12 cm, a fixed spray time of 5 minutes, and the process carried out at atmospheric pressure. The experimental conditions were optimized to ensure uniform deposition and high-quality films

• Here, we outline the diverse physical and chemical properties of the materials employed.

Table.III. 1: Summary of the Physical and Chemical Properties of the Materials Employed

Materials		Aluminum	
	Zinc acetate	chloride	Gallium Nitrate
Properties		hexahydrate	
Appearance	White crystalline solid with an acetic acid odor.	White or slightly yellow crystalline powder or colorless crystals	White Crystalline
Molecular	C H O Zn ·	Al(Cl□)·6H□O	$Ga(NO\square)\square \cdot 9H\square O$
formula	2Н□О		
Molecular	219.50 g/mol	241.33454 g/mol	255.74 g/mol
weight			
Solubility	soluble in water	Highly soluble in	soluble in water,
	and methanol	water	ethanol and diethyl ether
Density	1.735 g/ cm ³	2.48 g/cm ³	6.44g/cm ³
Melting point	237° C	190°C	110 °C (decomposition of the solid hydrate)
	Fire Actions and Action of the	ARAMINA OBITAL ARAMINA	

III.1.3.Experimental Setup Used

This system was designed at the Physics Laboratory and Thin Film Applications at the University of Biskra, using simple components that were modified in order to obtain homogeneous doped zinc oxide films Figure (III.1).1illustrates the experimental device used for the deposition of these films.

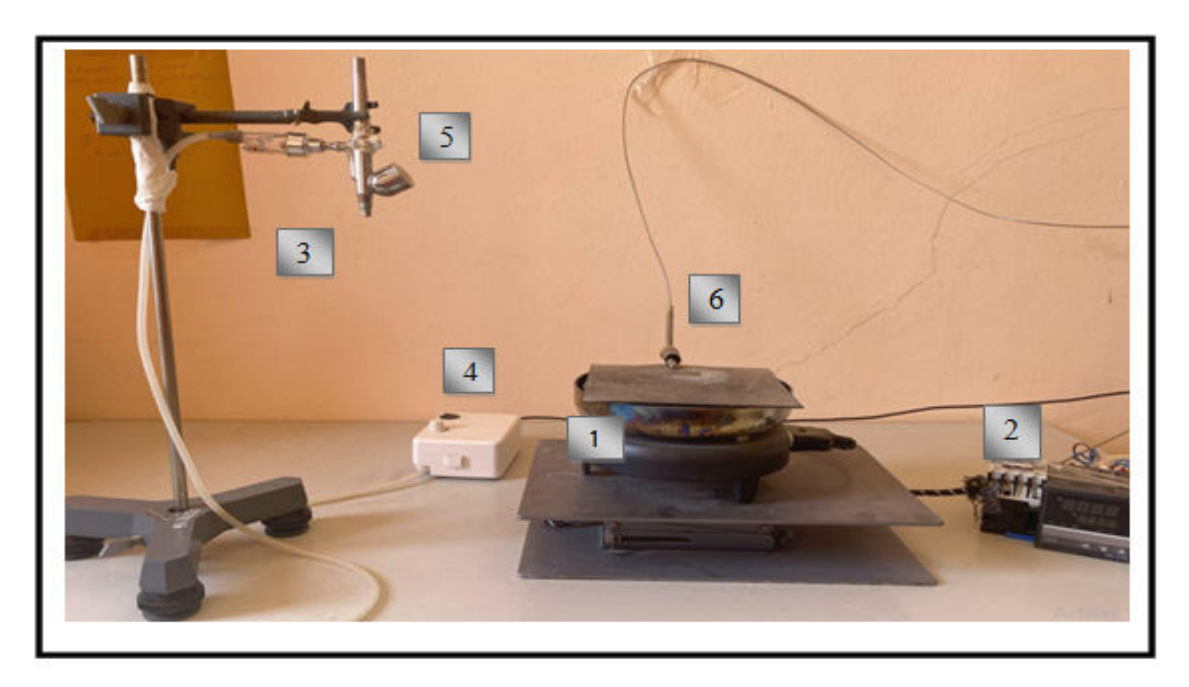


Figure (III.1): Image of the apparatus employed for deposition.

Deposition Device Components

The deposition setup consists of the following main components:

- **1.** Sample holder and heating plate.
- **2.** Temperature regulator connected with a thermocouple to check the temperature.
- **3.** Atomizer to decay the solution to fine droplets.
- **4.** Air compressor.
- **5.** Solution vial.
- **6.** Thermocouple.

III.2.Results and discussions

III.2.1.Crystal Structure Analysis Using X-ray Diffraction (XRD)

The following figure presents the X-ray diffraction (XRD) results of the studied samples, showing distinct crystalline peaks that reflect the material's crystal structure.

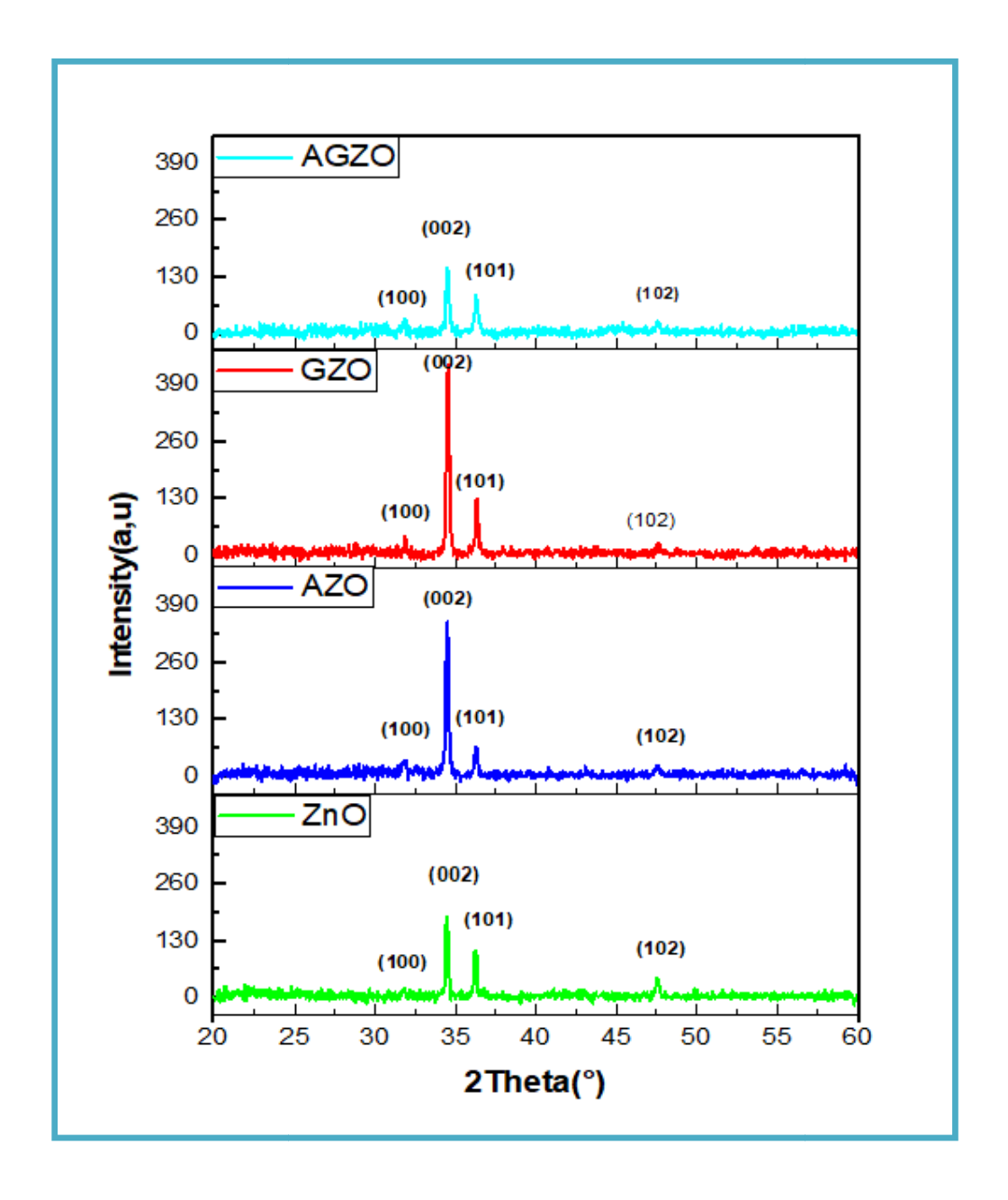


Figure (III.2): X-ray Diffraction Analysis of ZnO, AZO, GZO and AGZO Thin Films.

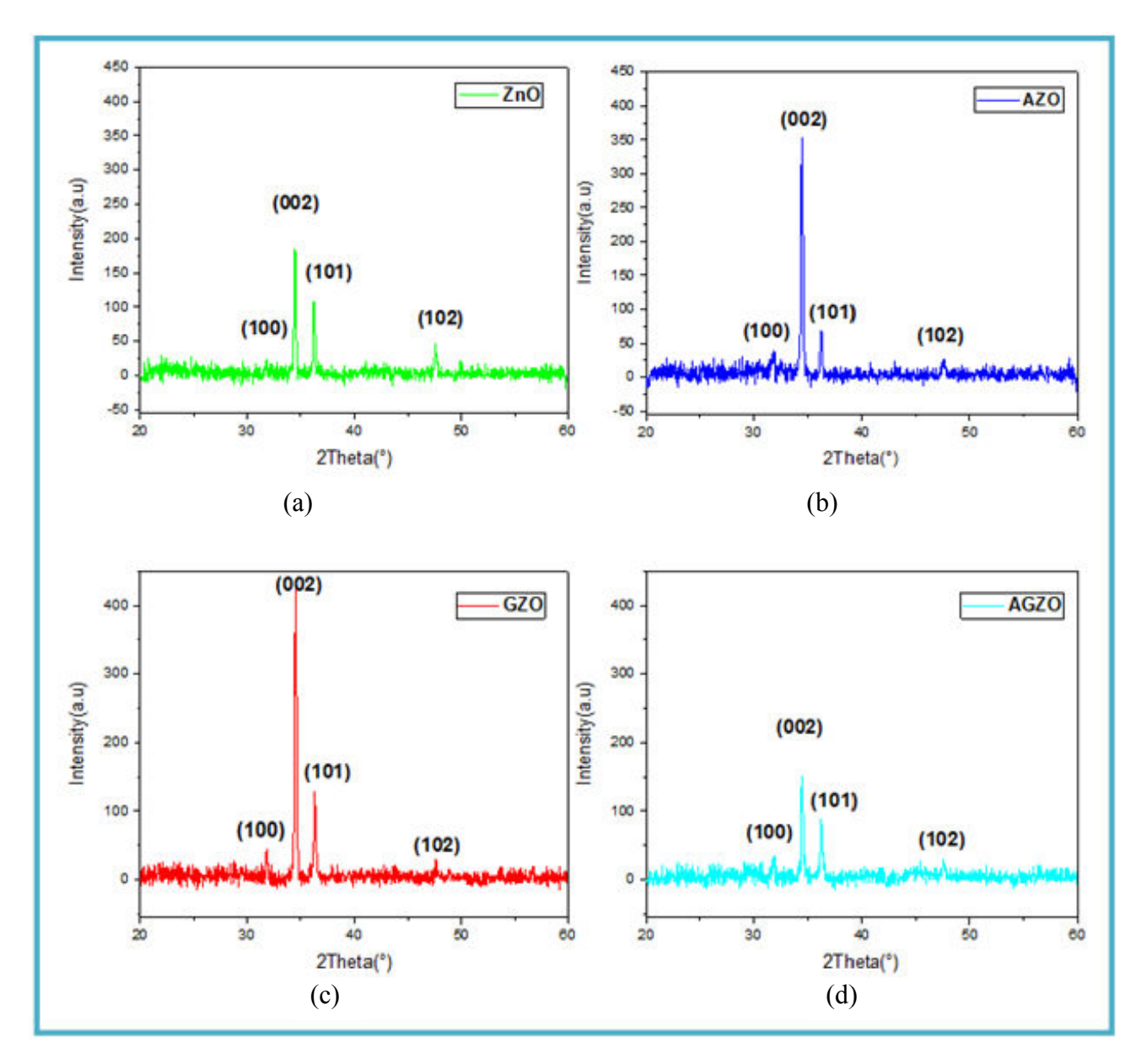


Figure III.3: X-ray diffraction patterns of ZnO thin films: (a) undoped ZnO, (b) Al-doped ZnO (AZO), (c) Ga-doped ZnO (GZO), and (d) Al/Ga co-doped ZnO (AGZO).

X-ray diffraction (XRD) analysis revealed distinct diffraction peaks, indicating the formation of a hexagonal wurtzite structure in the ZnO thin films(Figure.III.3). The diffraction peaks appeared clearly at 2θ angles of approximately 31.8° , 34.4° , 36.2° , and 47.5° , corresponding to the (100), (002), (101), and (102) crystallographic planes, respectively. These findings are consistent with numerous studies [1,2] and align with the reference data from JCPDS card No. 36-1451 [3].

Moreover, it is observed that the main peak at the 20 angle of 34.48°, corresponding to the (002) crystal plane, is very intense. This indicates that the crystallites are preferentially oriented along the c-axis, suggesting high crystalline quality and a well-aligned structure perpendicular to the substrate surface [4-6].No secondary phases (e.g., Al₂O₃ or Ga₂O₃) were detected in the XRD patterns. This suggests that aluminum and gallium ions either substitutionally replaced zinc in the lattice or occupied interstitial sites without forming impurity phases [7, 8].

Analysis of the (002) diffraction peaks shows a shift toward higher 20 values for AZO (34.4723°), GZO (34.5305°) and AGZO (34.4774°) compared to undoped ZnO (34.4709°), as shown in Figure (III.4). This shift confirms the substitutional incorporation of Al³⁺ and Ga³⁺ into the ZnO lattice. The smaller ionic radii of Al³⁺ (0.54 Å) and Ga³⁺ (0.62 Å), relative to Zn²⁺ (0.74 Å), lead to a reduction in lattice spacing (d_{hkl}) and alter the lattice parameters (Table III.2) [9].

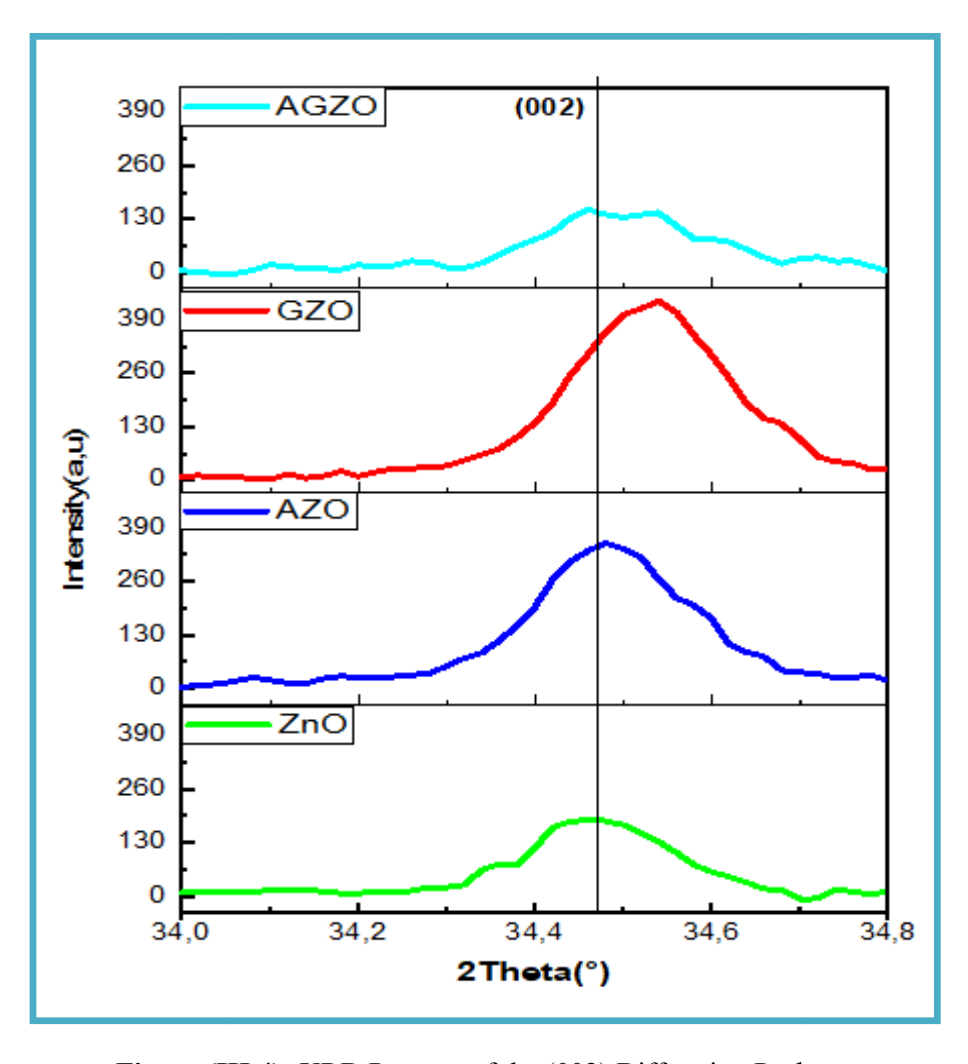


Figure (III.4): XRD Patterns of the (002) Diffraction Peak

Table (III.2): Structural Analysis of ZnO and Doped Samples.

Samp	ols	ZnO	AZO	GZO	AGZO
2θ (°)		34,4709	34,4723	34,5305	34,4774
(hkl)		(002)	(002)	(002)	(002)
d(hkl) (Å)		0,25997	0,25996	0,25953	0,25992
Crystallit D (nn		44,14368	63,04434	55,20254	44,14446
Strai ε (× 10		-1,0918	-1,1312	-2,7636	-1,2744
Dislocation density $\delta(\times 10^{14} lines/m^{-2})$		5,13	2,52	3,28	5,13
σ(GPc	a)	0,25417	0,47936	0,8590343	0,512682
Lattice constants	a	3,23631	3,23468	3,24048	3,23948
(Å)	c	5,19948	5,19927	5,19077	5,19852
c/a		1,6066	1.6073	1.6018	1.6047

According to Table (III.2), slight deviations are observed between the experimental results and the reference data from the JCPDS card for zinc oxide Based on the standard JCPDS data, the lattice parameters of ZnO are a_0 = 3.2499 Å and c_0 = 5.2052 Å[10]. In this study, the calculated lattice parameters (a and c) for undoped ZnO thin films are a = 3.2363 Å and c = 5.1995 Å Figure (III.5), which are slightly smaller than the standard values. These parameters further decrease upon doping with Al and Ga, as shown in Figure III.5. This reduction can be attributed to the substitution of Zn²⁺ ions by Al³⁺ and Ga³⁺ ions, which have smaller ionic radii, as previously discussed. Additionally, the positive stress values indicate tensile stress in the films, whereas the negative strain values suggest compressive strain [11]. These findings are consistent with previous studies [12].

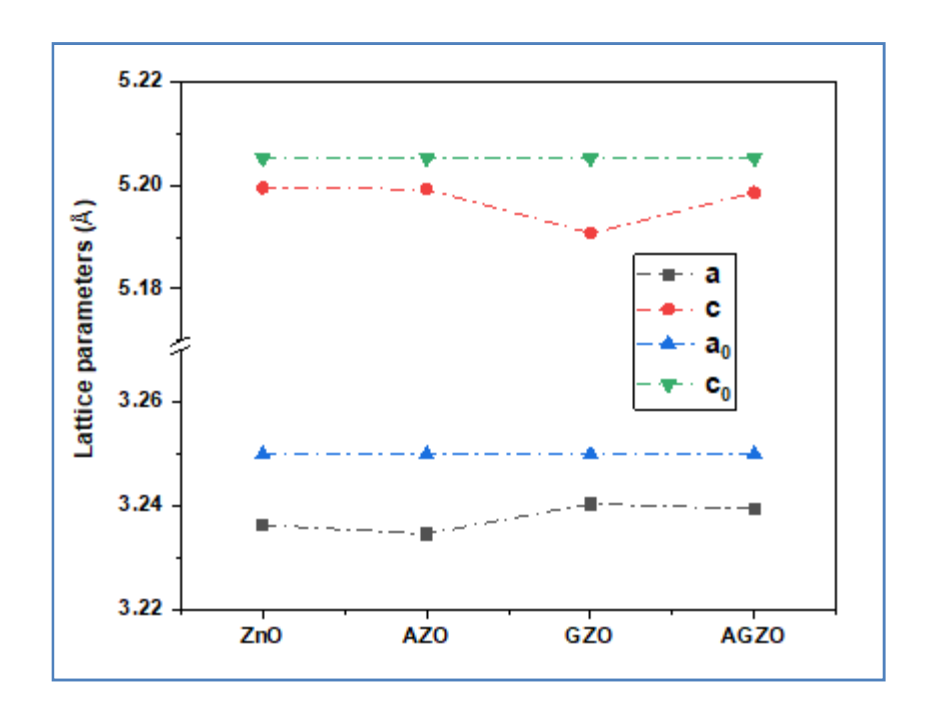


Figure (III.5): Variation of lattice parameters of undoped and doped ZnO thin films: ZnO, AZO, GZO, and AGZO.

III.2.1.1. Crystallite Size

The crystallite size was calculated using Scherrer's equation from the full width at half maximum (FWHM), and the results are presented in Table (III.2), and Figure (III.6)

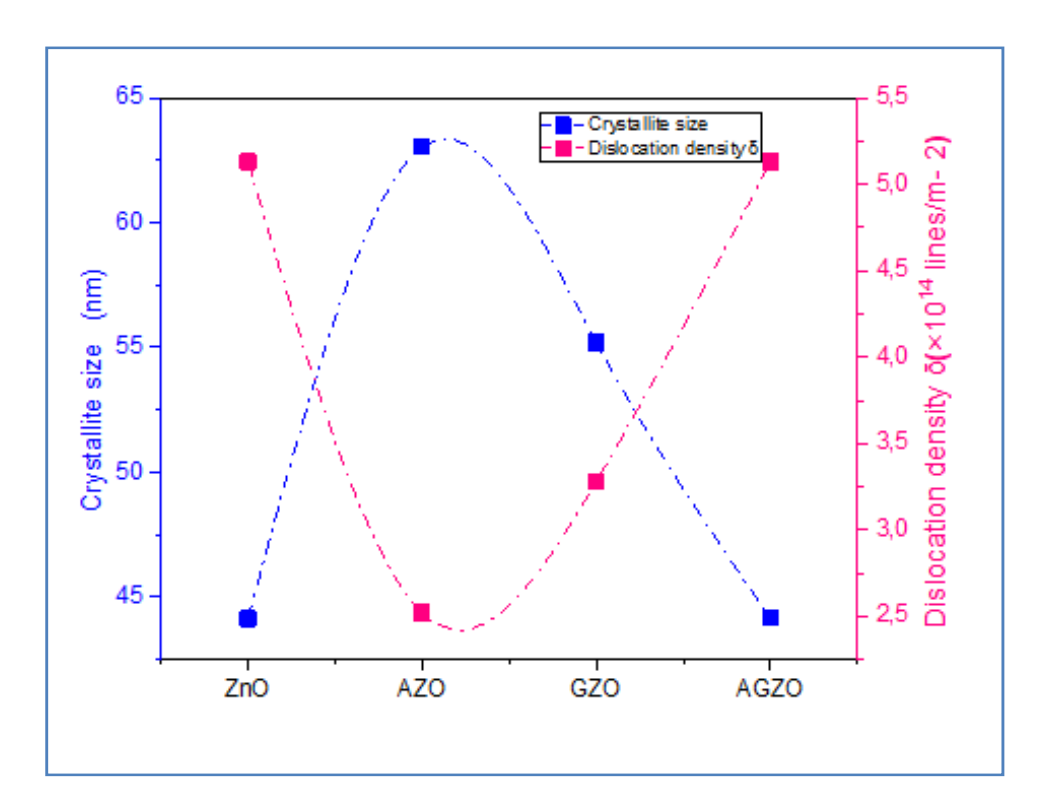


Figure (III.6): Variation in the crystallite size, dislocation density of ZnO, AZO, GZO, and AGZO samples.

The observed variations in crystallite size and dislocation density for the ZnO, AZO, GZO, and AGZO thin films reflect the influence of doping on the structural properties of ZnO. Dopants such as aluminum (Al) and gallium (Ga) can modify grain growth and defect formation during thin film deposition.

The undoped ZnO thin film exhibits a crystallite size of approximately 44 nm and a dislocation density of 5.13×10^{14} lines/m², indicating moderate crystallinity with a significant number of lattice defects. Upon doping with aluminum (AZO), the crystallite size increases significantly to about 63 nm, accompanied by a notable decrease in dislocation density to 2.52×10^{14} lines/m², suggesting improved crystallinity due to Al incorporation, which promotes grain coalescence and reduces grain boundary defects.

In contrast, gallium doping (GZO) results in a moderate crystallite size of approximately 55 nm and a dislocation density of 3.28×10^{14} lines/m², indicating enhanced but slightly inferior structural properties compared to AZO, likely due to differences in ionic radii and doping efficiency.

Interestingly, the co-doped AGZO sample exhibits a crystallite size similar to undoped ZnO (\sim 44 nm) and a dislocation density comparable to pure ZnO ($5.13 \times 10^{14} \, \text{lines/m}^2$). This suggests that co-doping with Al and Ga may introduce competitive or compensating effects, diminishing the beneficial impacts observed with single-element doping [13].

III.2.1.2.Film thickness

The calculated film thickness values for ZnO, AZO, GZO, and AGZO thin films are illustrated in Figure (III.7)

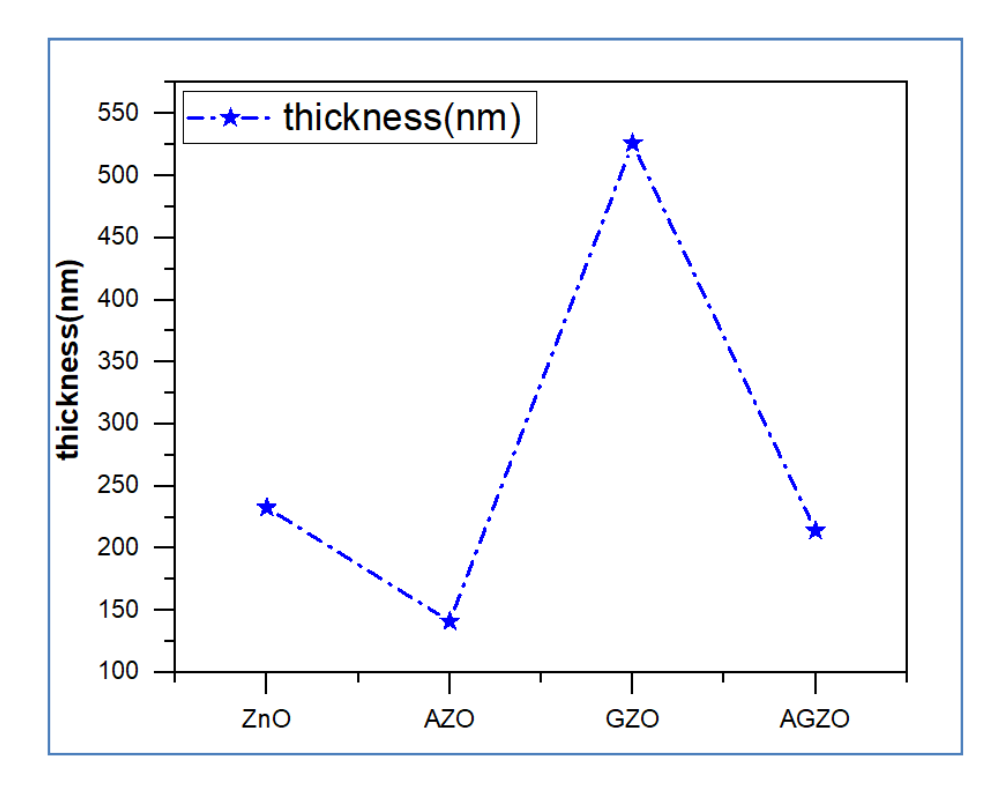


Figure (III.7): Film Thickness Variation in ZnO, AZO, GZO, and AGZO Thin Films.

Based on the thickness measurements in Figure (III.7), the GZO film is thicker than ZnO, AZO, and AGZO. The incorporation of gallium has a significant effect on the film thickness, reaching a maximum value of 526 nm. The XRD curve shows that the (002) peak for the GZO sample reached its maximum intensity, and the thickness also reached its highest value for this sample. This correlation between peak intensity and film thickness suggests that the observed changes are due to structural modifications induced by doping [14].

These observations align with the growth model transition reported by Garcés et al. [15], where thinner films typically follow 2D growth while thicker films transition to 3D growth modes. Our results suggest that gallium doping promotes this 2D-to-3D transition at

lower measured film thickness compared to undoped or other doped films.

III.2.2.Optical Analysis

This study investigates the transmittance, refractive index, and optical band gap to understand how doping and co-doping with Al and Ga affect the optical characteristics of ZnO films.

III.2.2.1.Transmittance Spectra:

The transmittance spectra of ZnO, AZO, GZO, and AGZO thin films were analyzed in the wavelength range of 300 to 800 nm, as shown in Figure (III.8).

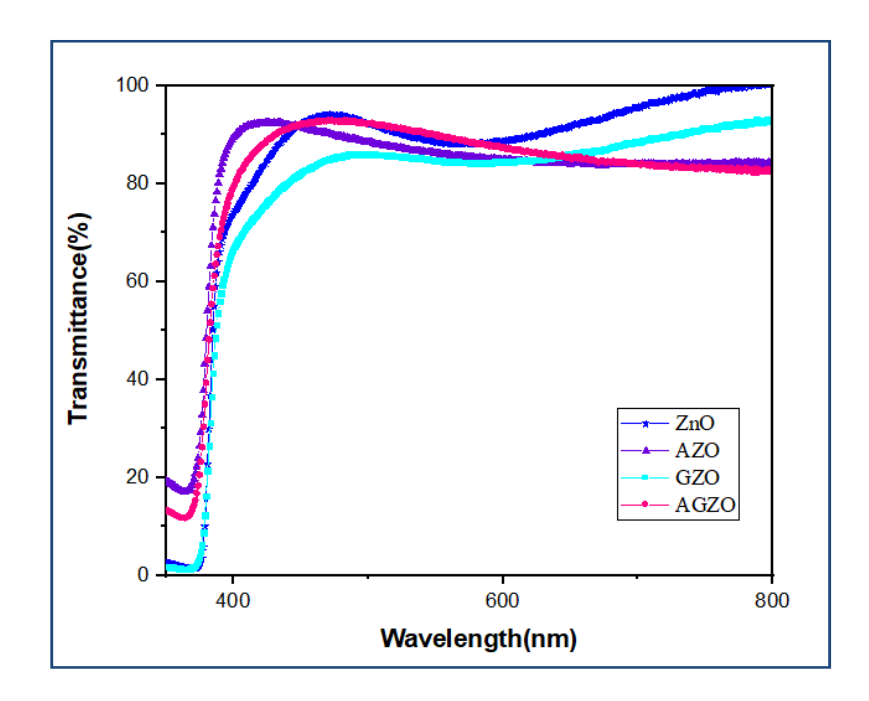


Figure (III.8): Optical Transmittance Spectrum of ZnO-Based Thin Films.

The films exhibited optical transmittance exceeding 85% in the visible region, with a sharp fundamental absorption edge [16], as shown in the transmittance curve. These curves demonstrate distinct variations in the films' response to light within this spectral range. A sharp increase in transmittance is observed at short wavelengths (380–400 nm), indicating the presence of an optical absorption edge caused by electronic transitions from the valence band to the conduction band. Beyond this edge, in the visible range (400–800 nm), transmittance stabilizes at different levels depending on the sample type, further reflecting the impact of dopant type on the material's optical behavior.

Undoped ZnO sample exhibited the highest transparency at longer wavelengths, making it suitable for applications requiring high transmittance. AZO performed well at the beginning of the visible range but showed a gradual decrease in transmittance with increasing wavelength. GZO exhibited the lowest transmittance, possibly due to its higher film thickness. It is well known that transmittance depends on sample thickness according to the Beer-Lambert law (see Chap. II). Therefore, an increase in film thickness leads to a decrease in optical transmittance.

Although dual doping may contribute to a slight reduction in optical transmittance due to decreased crystallinity, as confirmed by previous XRD results, and an increase in grain boundaries that enhances light scattering, the AGZO sample demonstrated superior performance. It exhibited stable and high transmittance across the visible range, likely due to its lower film thickness and reduced surface roughness.

III.2.2.2. Urbach Energy and Optical Band Gap:

The optical bandgap and Urbach energy of the ZnO thin films were calculated using the Tauc model and the Urbach tail method, respectively. The optical bandgap was determined by extrapolating the linear portion of the Tauc plot based on the relation (II. 10) This approach is consistent with previous studies that employed similar methods to evaluate the optical properties of ZnO thin films [17].

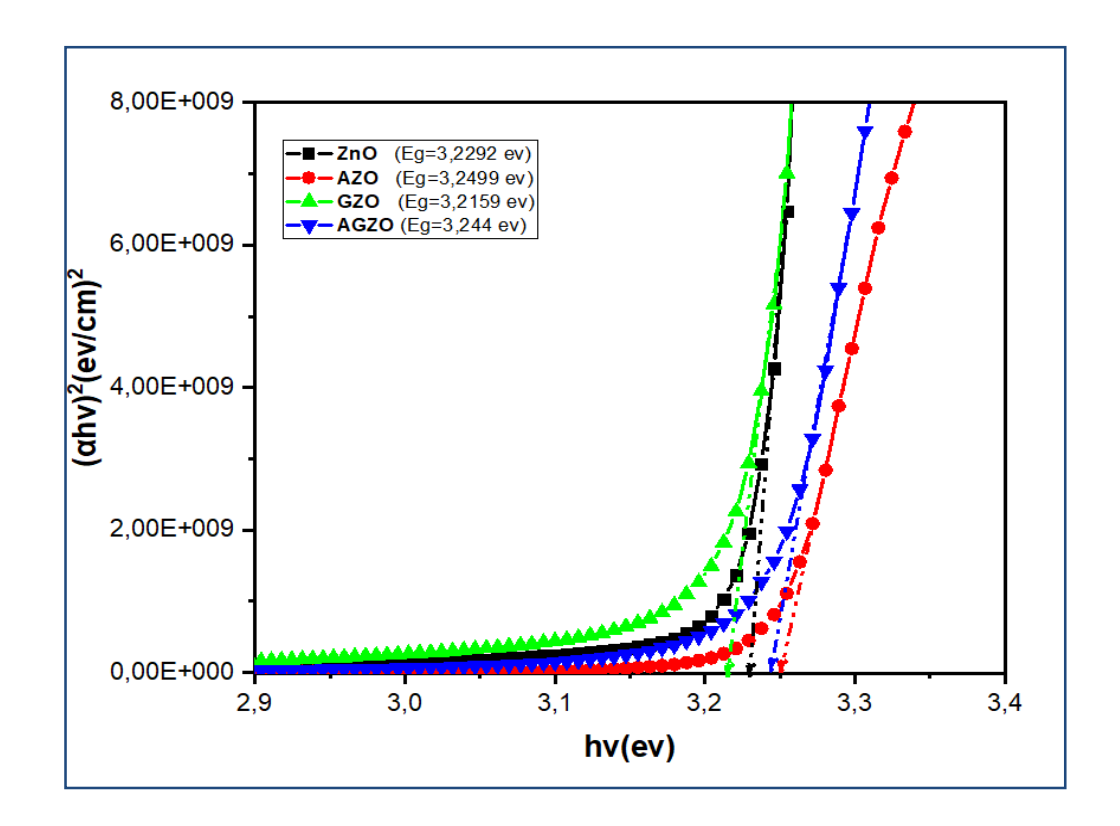


Figure (III.9): Variation of $(\alpha h \nu)^2$ with photon energy for ZnO, AZO, GZO, and AGZO samples.

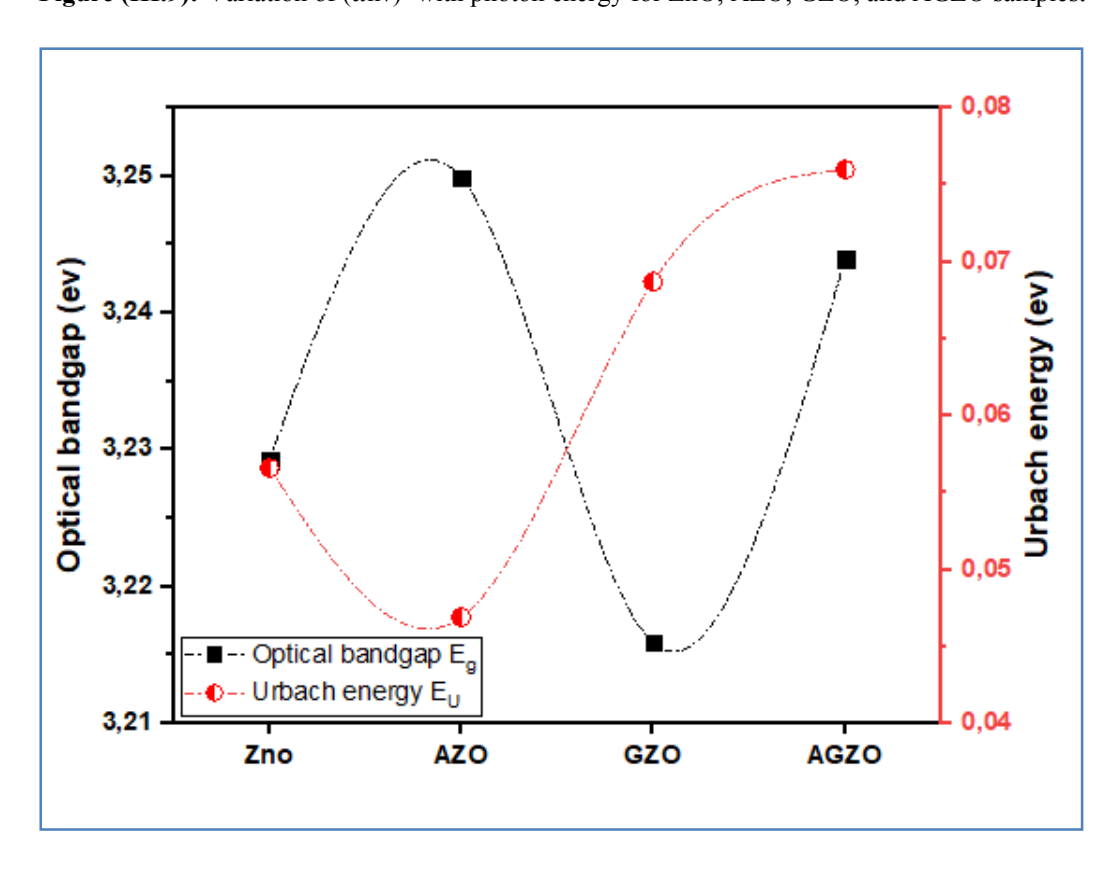


Figure (III.10): Variation of the band gap and Urbach energy of ZnO films.

52

Table (III.3) present the optical band gap, Urbach energy, and refractive index values for the prepared samples. The measured band gaps for ZnO, AZO, GZO, and AGZO thin films were 3.229, 3.25, 3.216, and 3.24 eV, respectively (Figure III.10). The optical band gap increases with the addition of Al or Al/Ga to the ZnO matrix. This increase can be attributed to the Burstein-Moss effect, which occurs because the Al or Al/Ga dopants enhance the carrier concentration. Substituting Al³⁺ or Ga³⁺ ions for Zn²⁺ in the ZnO structure introduces additional free electrons into the conduction band [18]. This increase in free carrier concentration causes electrons to occupy the lower energy states below the conduction band, effectively raising the Fermi level and widening the energy gap. Consequently, the band gap of ZnO films increases, in agreement with reported studies [15, 19-23].

The observed band gap for GZO films is lower than that of other samples, which can be attributed to the increased film thickness. Thicker films lead to localized states in the band structure that merge with the conduction band edges, resulting in a reduced band gap [24]. A similar effect has been observed in ZnO films [25].

Additionally, they [26, 27] explained the changes in the band gap through various mechanisms, including: (i) degradation of crystallinity, (ii) changes in crystallite size, (iii) quantum size effects, (iv) impurity density variations, and (v) strain-induced effects. Strain, which modifies the interatomic spacing (d_{hkl}) of semiconductors, can also affect the band gap, as demonstrated by Kamal Baba. This strain might explain the shift in the band gap observed in our films, as the strain increases with film thickness, as shown in Table III.2 and Figure III.7. On the other hand, the reduction in the band gap could also be attributed to the widening of the Urbach tail, which is associated with an increase in localized states.

Table (III.3) displays the refractive index values for ZnO, AZO, GZO, and AGZO thin films. The refractive index values calculated using the Ravindra relation are comparatively lower than those obtained using the Hervé–Vandamme method [28].

Table (III.3): Optical Parameters of ZnO-Based Thin Films: Band Gap, Urbach Energy, and Refractive Index Estimated Using Ravindra and Herve–Vandamme Models.

Sampls	Band Gap	Urbach energy Eu(ev)	Refractive index	
	Eg(ev)		Ravindra relation	Herve–Vandamme model
ZnO	3,2292	0,0566	2,0818	2,2822
AZO	3,2499	0,0469	2,0690	2,2765
GZO	3,2159	0,0687	2,0901	2,2859
AGZO	3,244	0,076	2,0723	2,2781

III.2.3. Electrical Characteristics

III.2.3.1.Resistivity

The following figure illustrates the variation in electrical resistivity of undoped and doped ZnO thin films (AZO, GZO, AGZO):

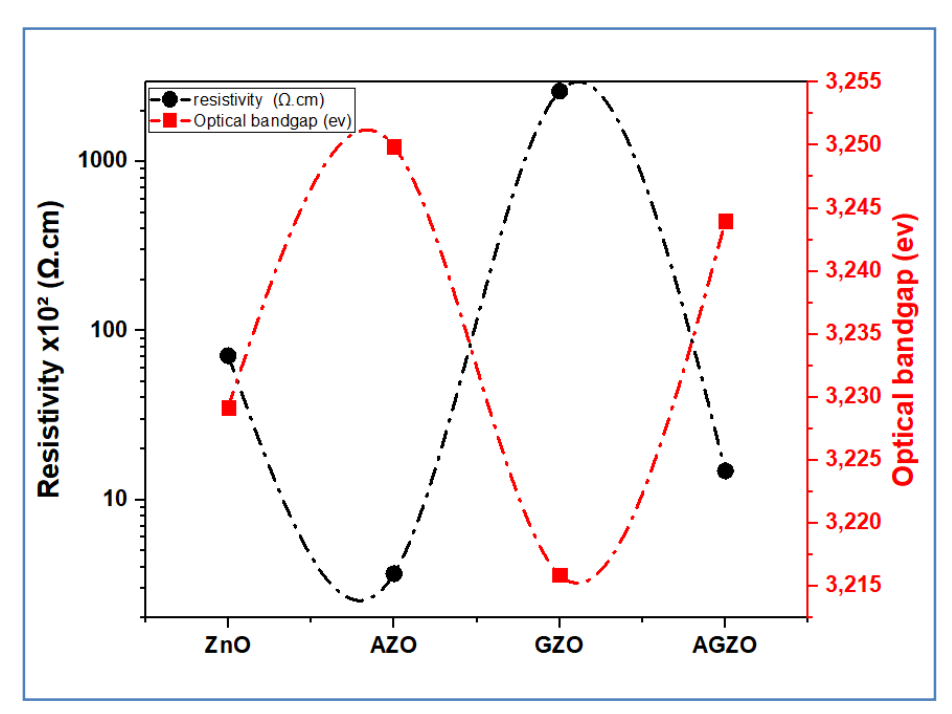


Figure (III.11): Variation of resistivity and optical band gap for different ZnO samples.

The resistivity of ZnO-based thin films is inversely related to their optical bandgap, influenced by doping-induced modifications in the electronic structure. The high resistivity (\sim 7110 Ω .cm) of undoped ZnO is attributed to its wide bandgap (\sim 3.23 eV), which limits the intrinsic carrier concentration [29]. Doping with aluminum (AZO) reduces resistivity (\sim 364 Ω .cm) by introducing shallow donor states that (1) increase the free-electron density and (2) slightly widen the bandgap (\sim 3.25 eV) via the Burstein-Moss effect, where an increased carrier population fills conduction band states, effectively pushing the bandgap upward (Minami) [30].

In contrast, Ga-doped ZnO (GZO) exhibits unusually high resistivity (\sim 2.6×10 \square Ω .cm), despite Ga being a donor. The nearly constant bandgap (\sim 3.22 eV), similar to that of undoped ZnO, suggests defect compensation mechanisms (e.g., Ga interstitials or Zn vacancies) that trap carriers, thereby disrupting the expected inverse relationship between bandgap and resistivity [31].

For AGZO, the intermediate resistivity (\sim 1480 Ω .cm) and bandgap (\sim 3.24 eV) reflect a balance between the effects of Al and Ga. Aluminum enhances conductivity, while defects associated with Ga partially counteract this effect, maintaining a moderate bandgap. Samavati et al [32] investigated the structural, optical, and electrical properties of Al–Ga co-doped ZnO (AGZO) thin films. They observed that co-doping with both aluminum and gallium resulted in improved crystallinity and enhanced electrical conductivity compared to singly doped films. The study also noted that the optical bandgap of AGZO films was slightly higher than that of pure ZnO, indicating a balance between the effects of Al and Ga dopants.

The figure of Merit (FOM) values for ZnO, AZO, GZO, and AGZO thin films were calculated to be approximately 1.49×10^6 , 8.85×10^6 , 4.45×10^4 , and 3.72×10^6 Ω^{-1} , respectively (Table III.4). These values indicate a significant enhancement in the electrical conductivity and optical transparency of AZO and AGZO films compared to undoped ZnO and GZO, consistent with Haacke's (1976) original FOM definition and subsequent studies [33]. The higher FOM values for AZO and AGZO films highlight the beneficial effects of aluminum doping and Al/Ga co-doping, which improve carrier concentration while reducing resistivity. In contrast, the lower FOM of GZO suggests less efficient charge transport, likely

due to incomplete dopant activation, lower solubility of Ga in ZnO, or defect compensation mechanisms.

Table III.4. Electrical parameters of ZnO, AZO, GZO and AGZO thin films .

Sampls	Average Transmittance	Sheet resistance Rs (Ω)	Figure of merit $(imes 10^4)(\Omega)^{-1}$
ZnO	0,9244021	3,05563E7	149,1
AZO	0,8627224	2,58076E6	885
GZO	0,8599404	4,96363E8	4,45
AGZO	0, 8731465	6,91571E6	372,4

References

- [1] Sandeep, K. M., Bhat, S., & Dharmaprakash, S. M. (2018). Nonlinear absorption properties of ZnO and Al doped ZnO thin films under continuous and pulsed modes of operations. *Optics & Laser Technology*, *102*, 147-152.
- [2] Ivanova, T., Harizanova, A., Koutzarova, T., Vertruyen, B., & Stefanov, B. (2018). Structural and morphological characterization of sol-gel ZnO: Ga films: Effect of annealing temperatures. *Thin Solid Films*, 646, 132-142.
- [3] Bett, K., & Kiprotich, S. (2024). Effects of stirring speed of precursor solution on the structural, optical, and morphological properties of ZnO:Al:Ga co-doped nanoparticles synthesized via a facile sol-gel technique. *American Journal of Condensed Matter Physics*, 13(1), 9–20.
- [4] Liu, J., Zhang, W., Song, D., Ma, Q., Zhang, L., Zhang, H., ... & Wu, R. (2013). Investigation of aluminum–gallium co-doped zinc oxide targets for sputtering thin film and photovoltaic application. *Journal of alloys and compounds*, 575, 174-182.
- [5] Shinde, S. S., Shinde, P. S., Pawar, S. M., Moholkar, A. V., Bhosale, C. H., & Rajpure, K. Y. (2008). Physical properties of transparent and conducting sprayed fluorine doped zinc oxide thin films. *Solid State Sciences*, *10*(9), 1209-1214.
- [6] Tüzemen, E. Ş., Eker, S., Kavak, H., & Esen, R. (2009). Dependence of film thickness on the structural and optical properties of ZnO thin films. *Applied Surface Science*, 255(12), 6195–6200.
- [7] Huang, L., Sun, Y., Li, M., Yi, Y., Jiang, L., & Fang, L. (2019). Sol-gel derived Al and Ga co-doped ZnO nanoparticles: Structural, morphological and optical investigation. *Optik*, 192, 162942.
- [8] Rao, T. P., & Kumar, M. S. (2010). Physical properties of Ga-doped ZnO thin films by spray pyrolysis. *Journal of Alloys and Compounds*, 506(2), 788-793.
- [9] Alsaad, A. M., Ahmad, A. A., Qattan, I. A., Al-Bataineh, Q. M., & Albataineh, Z. (2020). Structural, optoelectrical, linear, and nonlinear optical characterizations of dip-synthesized

undoped ZnO and group III elements (B, Al, Ga, and In)-doped ZnO thin films. *Crystals*, 10(4), 252.

- [10] Berramdane, F. (2024). *Influence of Mg doping on properties of Mg-Al co-doped ZnO thin films prepared by spray pyrolysis method* (Mémoire de master, Université Mohamed Khider de Biskra, Département des Scienc).
- [11] KABOT, O., & MERIZIG, M. (2022). L'effet de la température de recuit sur les propriétés des couches minces de ZnO: Al déposées par spray pneumatique(*Mémoire de master, Université Mohamed Khider de Biskra*).
- [12] Li, C., Li, X. C., Yan, P. X., Chong, E. M., Liu, Y., Yue, G. H., & Fan, X. Y. (2007). Research on the properties of ZnO thin films deposited by using filtered cathodic arc plasma technique on glass substrate under different flow rate of O2. *Applied Surface Science*, 253(8), 4000-4005.
- [13] Huang, L., Sun, Y., Li, M., Yi, Y., Jiang, L., & Fang, L. (2019). Sol-gel derived Al and Ga co-doped ZnO nanoparticles: Structural, morphological and optical investigation. *Optik*, 192, 162942.
- [14] Ajili, M., Jebbari, N., Turki, N. K., & Castagné, M. (2012). Effect of Al-doped on physical properties of ZnO Thin films grown by spray pyrolysis on SnO2: F/glass. In *EPJ Web of conferences* (Vol. 29, p. 00002). EDP Sciences.
- [15] Garcés, F. A., Budini, N., Arce, R. D., & Schmidt, J. A. (2015). Thickness dependence of crystalline structure of Al-doped ZnO thin films deposited by spray pyrolysis. *Procedia Materials Science*, *9*, 221-229.
- [16] Jun, M. C., Park, S. U., & Koh, J. H. (2012). Comparative studies of Al-doped ZnO and Ga-doped ZnO transparent conducting oxide thin films. *Nanoscale research letters*, 7, 1-6.
- [17] Shou, C., Yang, T., Ren, K., Almujtabi, A., Zhu, E., Mahmud, Q. S., ... & Liu, J. (2025). Photoluminescence study of optical transitions in spinel zinc gallium oxide thin films. *Scientific Reports*, *15*(1), 1-10.
- [18] Akdağ, A., Budak, H. F., Yılmaz, M., Efe, A., Büyükaydın, M., Can, M., ... & Sönmez, E. (2016, April). Structural and morphological properties of Al doped ZnO nanoparticles. In *Journal of Physics: Conference Series* (Vol. 707, No. 1, p. 012020). IOP Publishing.

- [19] Srinatha, N., Raghu, P., Mahesh, H. M., & Angadi, B. (2017). Spin-coated Al-doped ZnO thin films for optical applications: Structural, micro-structural, optical and luminescence studies. *Journal of Alloys and Compounds*, 722, 888-895.
- [20] Iqbal, J., Jan, T., Ismail, M., Ahmad, N., Arif, A., Khan, M., ... & Arshad, A. (2014). Influence of Mg doping level on morphology, optical, electrical properties and antibacterial activity of ZnO nanostructures. *Ceramics International*, 40(5), 7487-7493.
- [21] Majeed, M. H., Aycibin, M., & Imer, A. G. (2022). Study of the electronic, structure and electrical properties of Mg and Y single doped and Mg/Y co-doped ZnO: Experimental and theoretical studies. *Optik*, 258, 168949.
- [22] Kumar, P., Malik, H. K., Ghosh, A., Thangavel, R., & Asokan, K. (2013). Bandgap tuning in highly c-axis oriented Zn1–xMgxO thin films. *Applied Physics Letters*, 102(22).
- [23] Wu, W. C., & Juang, Y. D. (2022). The optical properties of Mg-doped ZnO quantum dots. *Solid State Communications*, *350*, 114791.
- [24] Baba, K., Lazzaroni, C., & Nikravech, M. (2015). ZnO and Al doped ZnO thin films deposited by Spray Plasma: Effect of the growth time and Al doping on microstructural, optical and electrical properties. *Thin Solid Films*, 595, 129-135.
- [25] Mariappan, R., Ponnuswamy, V., Suresh, P., Ashok, N., Jayamurugan, P., & Bose, A. C. (2014). Influence of film thickness on the properties of sprayed ZnO thin films for gas sensor applications. *Superlattices and Microstructures*, 71, 238-249.
- [26] Thilakan, P., & Kumar, J. (1997). Studies on the preferred orientation changes and its influenced properties on ITO thin films. *Vacuum*, 48(5), 463-466.
- [27] Thilakan, P., & Kumar, J. (1998). Oxidation dependent crystallization behaviour of IO and ITO thin films deposited by reactive thermal deposition technique. *Materials Science and Engineering: B*, 55(3), 195-200.
- [28] Hamani, N., Bourhefir, R., Hafaifa, L., Bennaceur, K., & Berramdane, F. (2024). Influence of Al and Mg co-doping on structural and optical properties of ZnO thin films deposited by spray pyrolysis. *Journal of Optics*, 1-11.

- [29] Özgür, Ü., Alivov, Y. I., Liu, C., Teke, A., Reshchikov, M. A., Doğan, S., ... & Morkoç, A. H. (2005). A comprehensive review of ZnO materials and devices. *Journal of applied physics*, 98(4).
- [30] Minami, T. (2005). Transparent conducting oxide semiconductors for transparent electrodes. *Semiconductor science and technology*, 20(4), S35.
- [31] Look, D. C., Reynolds, D. C., Sizelove, J. R., Jones, R. L., Litton, C. W., Cantwell, G., & Harsch, W. C. (1998). Electrical properties of bulk ZnO. *Solid state communications*, 105(6), 399-401.
- [32] Samavati, A., Samavati, Z., Ismail, A. F., Othman, M. H. D., Rahman, M. A., Zulhairun, A. K., & Amiri, I. S. (2017). Structural, optical and electrical evolution of Al and Ga codoped ZnO/SiO□/glass thin film: Role of laser power density. *RSC Advances*, 7(49), 30714–30722.
- [33] Haacke, G. (1976). New figure of merit for transparent conductors. *Journal of Applied physics*, 47(9), 4086-4089.

General Conclusion

In this work, thin films of ZnO, AZO, GZO, AGZO were prepared using the chemical spray pyrolysis (CSP) technique. These films were subjected to several characterization techniques, including X-ray diffraction (XRD) for structural analysis, ultraviolet-visible (UV-Vis) spectrophotometry for optical property evaluation, and finally, the four-point probe method to measure the electrical resistivity.

- ➤ Structural analysis using X-ray diffraction (XRD) revealed that all prepared samples exhibited a hexagonal wurtzite structure with a preferred orientation along the (002) plane, indicating high crystalline quality. The crystallite size varied depending on the type of doping, with aluminum-doped samples (AZO) showing the largest crystallite size (~63 nm), followed by galium-doped samples (GZO), while the undoped (ZnO) and co-doped (AGZO) samples exhibited intermediate crystallite size (~44 nm). These variations are related to doping effects on lattice distortions and film quality.
- ➤ The optical study revealed that the prepared thin films of ZnO, AZO and AGZO exhibit high optical transmittance exceeding 85% in the visible region. In contrast, the GZO sample recorded slightly lower transmittance, likely due to its increased thickness.
 - The optical band gap (Eg) ranged from 3.216 eV (for GZO) to 3.25 eV (for AZO), which is attributed to the Burstein-Moss effect resulting from increased free carrier concentration.
- The electrical study of ZnO-based thin films revealed that AZO exhibited the most favorable electrical properties, with the lowest resistivity (\sim 364 Ω ·cm) and the highest figure of merit (FOM) (\sim 8.85×10 \square Ω^{-1}). In contrast, GZO showed high resistivity (\sim 2.6×10 \square Ω ·cm) and a low FOM (\sim 4.45×10 \square Ω^{-1}), likely due to defect compensation effects. AGZO presented a balanced performance, with moderate resistivity (\sim 1480 Ω ·cm) and a satisfactory FOM (\sim 3.72×10 \square Ω^{-1}). These results confirm that AZO and AGZO films are the most promising for optoelectronic applications such as solar cells.

Abstract

This study investigates the structural, optical, and electrical properties of thin films of undoped ZnO, Al-doped ZnO (AZO), Ga-doped ZnO (GZO), and Al/Ga-co-doped ZnO (AGZO) deposited using the pneumatic spray technique. Various characterization methods were employed, including X-ray diffraction (XRD) for crystal structure analysis, UV–visible spectrophotometry for optical properties, and the four-point probe technique for electrical resistivity measurements.

Keywords: ZnO thin film, (Al, Ga) doping, pneumatic spray, structural properties, optical and electrical properties.

الملخص

تهدف هذه الدراسة إلى التحقيق في الخصائص البنيوية والبصرية والكهربائية لأغشية رقيقة من أكسيد الزنك (ZnO) غير المشوب، والمشوب بالألمنيوم (AZO) ، والمشوب بالغاليوم (GZO)، والمشوب بكلا العنصرين معًا (AGZO) ، والمحضرة باستخدام تقنية الرش الهوائي (Pneumatic Spray). وقد تم استخدام عدة تقنيات في توصيف هذه الأغشية، شملت حيود الأشعة السينية (XRD) لتحليل البنية البلورية، والمطيافية فوق البنفسجية المرئية (UV-Vis) لدراسة الخصائص البصرية، بالإضافة إلى تقنية المجس الرباعي لقياس المقاومية الكهربائية.

أظهرت النتائج أن جميع الأغشية المترسبة تمتلك بنية بلورية من النوع السداسي (ورتزيت) مع تفضيل واضح للنمو على مستوى (002). كما أظهرت الأغشية نفاذية بصرية عالية تجاوزت 85% ضمن نطاق الطيف المرئي. أما الخصائص الكهربائية، فقد تباينت المقاومية بين العينات بشكل ملحوظ، حيث سجّل غشاء AZO أدنى قيمة مقاومية (~ 364 أوم.سم) وأعلى قيمة لمعيار الأداء ($\sim 10 \times 8.85$ أوم.سم) وأعلى فيمة مقابل، أظهر غشاء GZO مقاومية مرتفعة ($\sim 10 \times 8.85$ أوم.سم) وقيمة منخفضة لمعيار الأداء. أما غشاء AGZO فقد أبدى أداءً متوازئًا بمقاومية متوسطة (~ 1480 أوم.سم) ومعيار أداء مقبول ($\sim 1.0 \times 10.0 \times 10$

الكلمات المفتاحية الغشاء الرقيق لأكسيد الزنك (ZnO)، التشويب بالألمنيوم والغاليوم، تقنية الرش الهوائي، الخصائص البنيوية، الخصائص البصرية والكهربائية.

REPUBLIQUE ALGERIENNE DEMOCRATIQUE ET POPULAIRE MINISTERE DE L'ENNEIGNEMENT SU PERIEUR ET DE LA RECHERCHE SCIENTIFIQUE UNIVERSITE MOHAMED KHIDER - BISKRA

الجمهورية الجزائرية الديمقراطية الشعبية وزارة التعليم العالي والبحث العلمي جامعة مدرك خيرضر عسكرة كلية العلوم الديتينية

Faculté des SE

Département des Sciences de la matière

قسم: علوم المادة

Filière: Physique

تصريح شرفيي

بالالتزام بقواعد النزاهة العلمية لإنجاز بحث

(ملحق القرار 1082 المؤرخ في 2021/12/27)

أنا الممضي أسفله،

			=
			السيد(ة):
سنة تَانبِهُ ماستر	الصفة: طالب	قِبرَ مِارِ عِدا لِهِ والدِدِ	تخصص:ع
2025/02/149	٩٨٨٠٦ الصادرة بتاريخ	اقة التعريف الوطنية رقم: 8.1.	الحامل(ة) لبط
	سم: علوم الما ده	علمه ٢ الدقيقة ق	المسجل بكلية:
4		ر أعمال بحث : مذكرة	والمكلف بانجاز
Investiga	tion of the effects	of Al, Gazand AllGa	عنوانها:
co-doping on U	re proper ties of Zuc	O thin films prepared by	Spray Durolusis

أصرح بشرفي أني ألتزم بمراعاة المعايير العلمية والمنهجية ومعايير الأخلاقيات المهنية والنزاهة الأكاديمية المطلوبة في انجاز البحث المذكور أعلاه وفق ما ينص عليه القرار رقم 1082 المؤرخ في 2021/12/27 المحدد للقواعد المتعلقة بالوقاية من السرقة العلمية ومكافحتها.

التاريخ: 20\06\02.08.

إمضاء المعنى بالأمر